Theses and Dissertations   1. Thesis and Dissertation Collection, all items

1955

The emissivity of hydrogen atoms at high temperatures.

Benton, William C.

California Institute of Technology

http://hdl.handle.net/10945/14143

THE EMISSIVITY OF HYDROGEN ATOMS
AT HIGH TEMPERATURES

William C. Benton

THE EMISSIVITY OF HYDROGEN ATOMS

AT HIGH TEMPERATURES

Thesis by

William C. Benton

, U. S. Marine Corps

In Partial Fulfillment of the Requirements

For the Degree of

Aeronautical Engineer

California Institute of Technology

Pasadena, California

1955

THE EMISSIVITY OF HYDROGEN ATOMS
AT HIGH TEMPERATURES

Thesis by

William C. Benton

Major, U. S. Marine Corps

In Partial Fulfillment of the Requirements

For the Degree of

Aeronautical Engineer

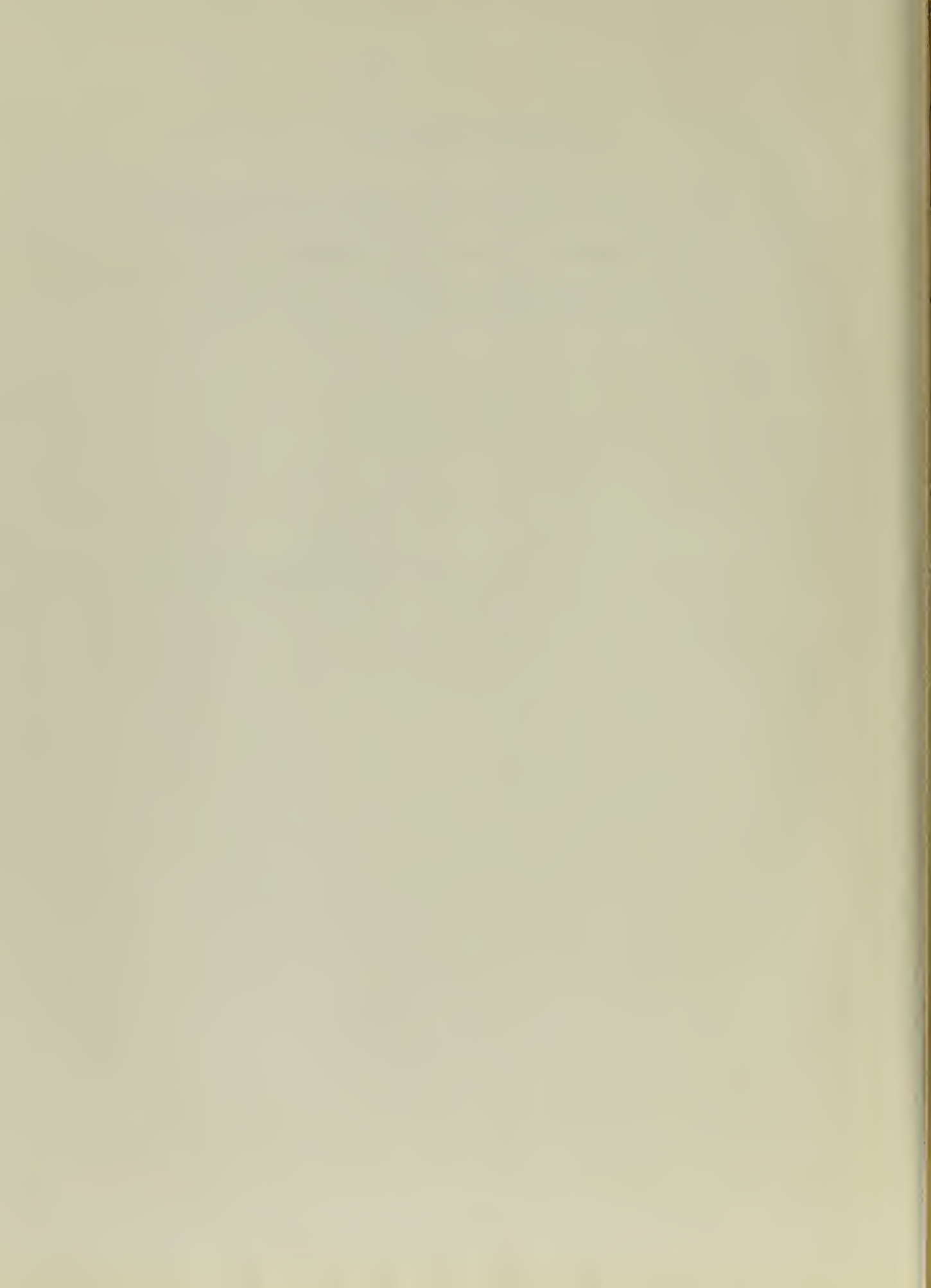California Institute of Technology

Pasadena, California

1955

ACKNOWLEDGEMENT

ii

ABSTRACT

A method is described for making estimates of the total emissivity of hydrogen in the temperature and pressure ranges where hydrogen atoms predominate under equilibrium conditions. For a characteristic geometrical depth of 50 cm, and temperatures of the order of $12,500^{\circ}$K and higher, with pressures of the order of 100 atmos and higher, the emissivity approaches unity ($\epsilon \gtrsim 0.95$), while for temperatures of the order of 9500°K and lower, with pressures of the order of 10 atmos and lower, the emissivity approaches zero ($\epsilon \lesssim 0.05$). The variations of the emissivity between these approximate limits are shown graphically as functions of temperature and pressure with the geometrical depth set at 50 cm. The variation of the emissivity with geometrical depth is also shown graphically at $12,600^{\circ}$K and 20 atmos.
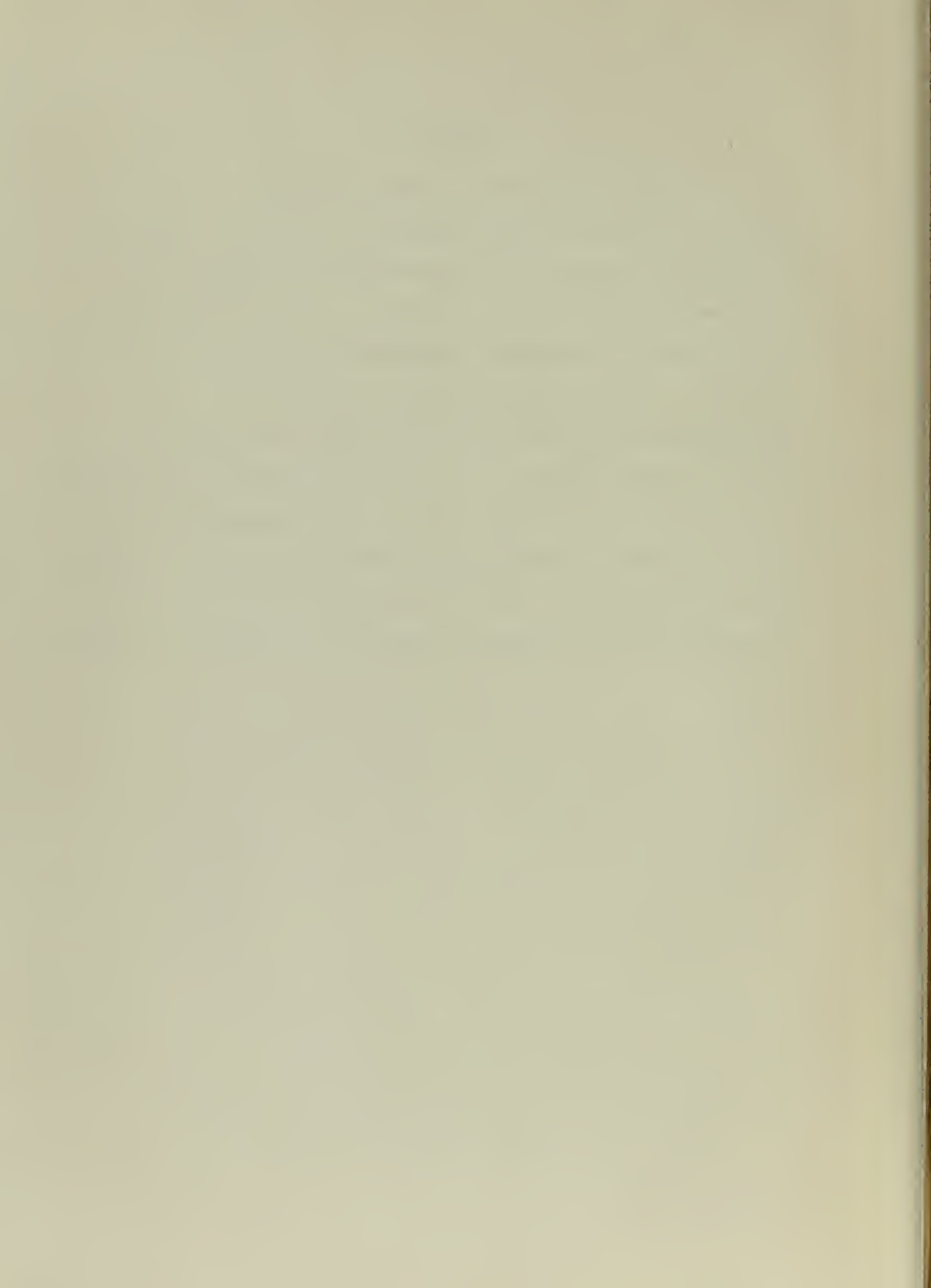
TABLE OF CONTENTS
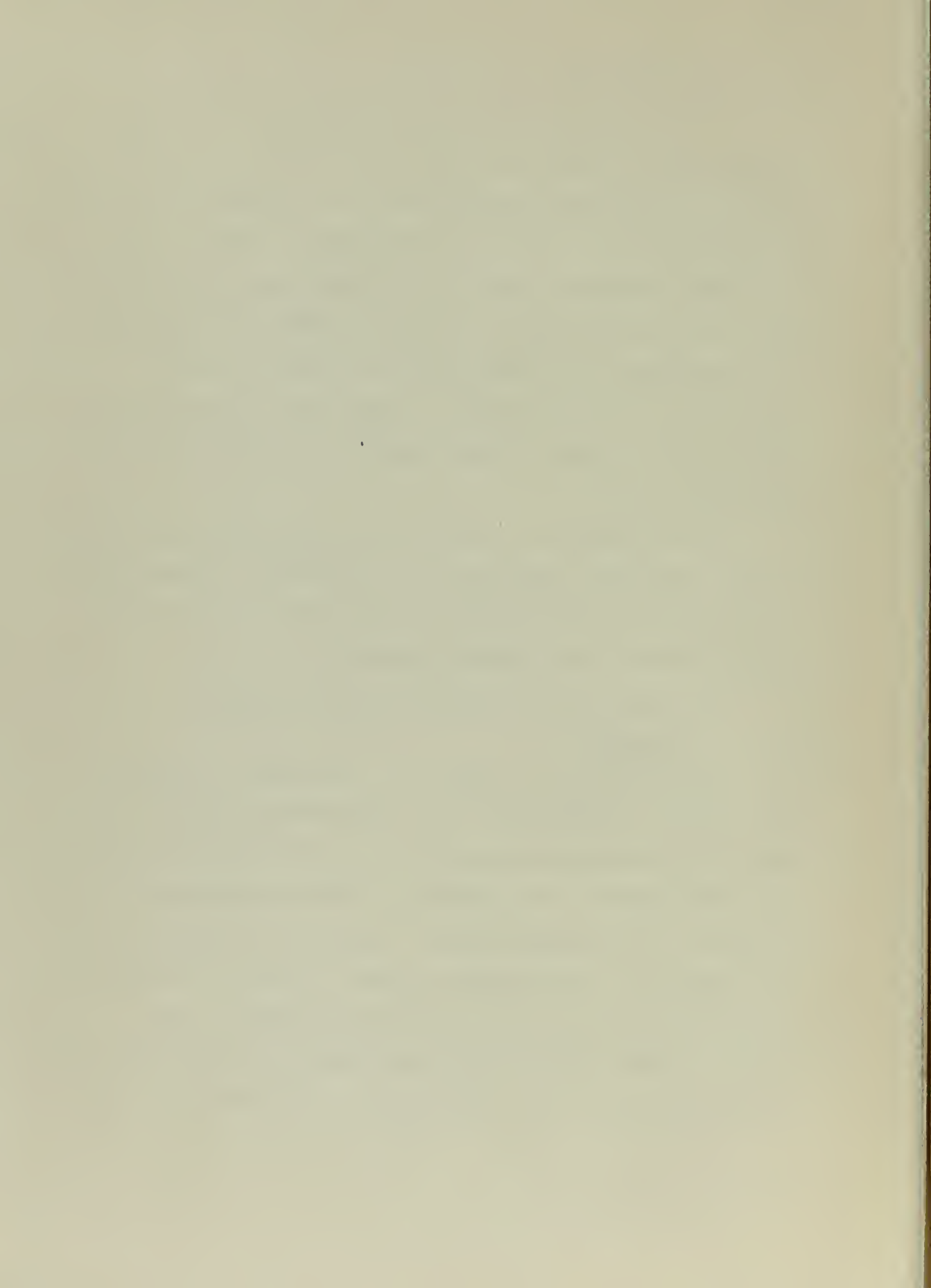
I.   INTRODUCTION

A rocket utilizing nuclear energy with hydrogen as working fluid has been considered in the past. It is therefore of some interest to obtain the emissivity of hydrogen atoms as a function of temperature and pressure in order to assess the importance of radiant heat transfer for high-temperature systems utilizing hydrogen. If the temperatures are sufficiently high, the hydrogen will exist almost completely in the atomic state, and hydrogen atoms will make the major contribution to the total emissivity. Furthermore, the treatment for hydrogen atoms provides a simple example of emissivity calculations for atomic systems.

The emissivity, ϵ , of a body is the ratio of the emitted radiant energy to the radiant energy emitted by a blackbody. The contributions to the emissivity of hydrogen atoms come from two sources: the continuous spectrum and the discrete transitions.

The blackbody curves may be obtained by plotting

$$R^{\circ}_{\omega} = \frac{2\pi\,\hbar c^2/\omega^3}{\exp(\hbar c\omega/kT) - 1}$$

against ω for various temperatures. Here $R^{\circ}_{\omega}\,d\omega$ (erg/cm^2-sec) is the radiant energy emitted by a blackbody, per unit area, per unit time, in the wave number interval $d\omega$ (cm^{-1}), into a solid angle of 2π steradians, $T(^{\circ}K)$ is the absolute temperature, c (cm/sec) is the velocity of light, $\hbar$ (erg-sec) is Planck's constant, and k (erg/$^{\circ}$K) is the Boltzmann constant. If one considers the system of heated hydrogen atoms to be isothermal and uniform, then $R_{\omega} = R^{\circ}_{\omega}\,[1 - \exp(-P_{\omega}X)]$. This function can be plotted as a function of ω on the same graphs as R°_{ω} . Here $R_{\omega}d\omega$ (erg/cm^2-sec) is the radiant

energy emitted by the hydrogen atoms, per unit area, per unit time, in
the wave number interval $d\omega$, into a solid angle of 2π steradians,
P_ω $(cm^{-1}$-atmos$^{-1})$ is the spectral absorption coefficient, and
X (cm-atmos) is the optical density. The spectral absorption coefficient
P_ω is set equal to $P_\omega^d + P_\omega^c$, where P_ω^d arises from discrete
transitions and P_ω^c from continuous spectrum contributions. To
obtain the emissivity one takes the ratio of the actual area under the
R_ω vs. ω curve to the blackbody area, σT^4, where
$\sigma = 5.6699 \times 10^{-5}$ erg/cm^2-$^\circ$K^4-sec. Examples of plots of R_ω and
R_ω° as functions of ω are reproduced in Figs. 1 to 5 for various
temperatures at a representative pressure of 40 atmos. For conven-
ience of presentation, $R_\omega^\circ / R_{\omega,max}^\circ$ and $R_\omega / R_{\omega,max}^\circ$ have been used as
ordinates, where $R_{\omega,max}^\circ$ is the maximum value of R_ω° . The con-
siderations used for the calculation of P_ω and hence R_ω will now
be described.

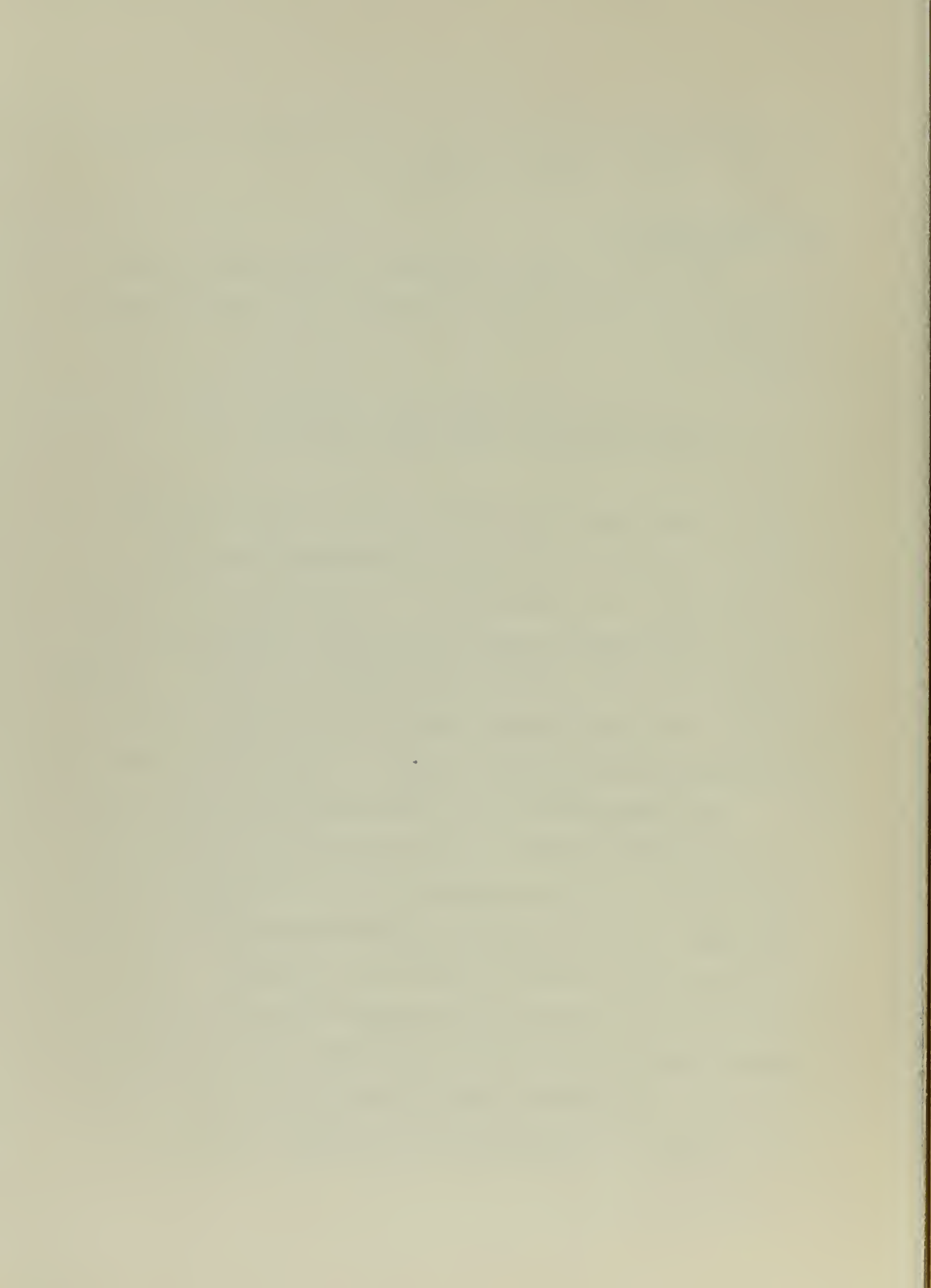## II. EVALUATION OF THE SPECTRAL ABSORPTION COEFFICIENT, P_ω , AND OF OPTICAL DENSITY, X .

A. Calculation of P_ω

The mass absorption coefficient in cm^2 per gram of neutral hydrogen atoms for the continuous spectrum, χ_ν' , has been given by Unsöld[1] as

$$\chi_\nu' = \frac{6 + \pi^4 m \, q^{10} \, e^{-u_1}}{3\sqrt{3} \, c \, h^3 \, m_H \, k^3 \, T^3 \, u^3} \left\{ \sum_{u_n < u}^{u_4} \frac{e^{u_n}}{n^3} + \frac{e^{u_5}}{2 u_1} \right\} (1 - e^{-u}). \tag{1}$$

Here m is the mass of the electron (g), q is the charge of the electron (esu), m_H is the mass of the hydrogen atom (g), $u = hc\omega/kT$, $u_n = Rhc/n^2 kT$, R is the Rydberg constant (cm^{-1}), and n is the principal quantum number of the hydrogen atom. To convert χ_ν' to P_ω^c , which has the units of cm^{-1}-$atmos^{-1}$, one must multiply by the atomic weight of hydrogen and divide by the absolute temperature and the molar gas constant, R' , in cm^3-atmos/mole-$^\circ$.

The contribution of the K'th spectral line whose center lies at ω_0 can generally be determined by computing the maximum value of $R_\omega(K) = R_{max}(K)$, which is usually the value of $R_\omega^2(K)$ at the line center [$\equiv R_{\omega_0}^\circ(K)$] and multiplying this quantity by the intensity width defined as the wave number range for which $R_\omega(K) \geq \frac{1}{2} R_{max}(K)$. Detailed calculations have shown that this procedure will give only an error of approximately one percent for the contribution of the line to the total emissivity. For collected methods of computing the spectral absorption coefficient of isolated lines see, for example, Penner and

Kavanagh[2]. The maximum absorption coefficient for purely Doppler broadened lines, P', is given by the equation

$$P' = (S/\omega_0)(m_H c^2/2\pi k T)^{1/2},$$ (2)

where S $(cm^{-2}$-$atmos^{-1})$ is the integrated intensity of the spectral line under consideration. The integrated intensity, S, may be written as
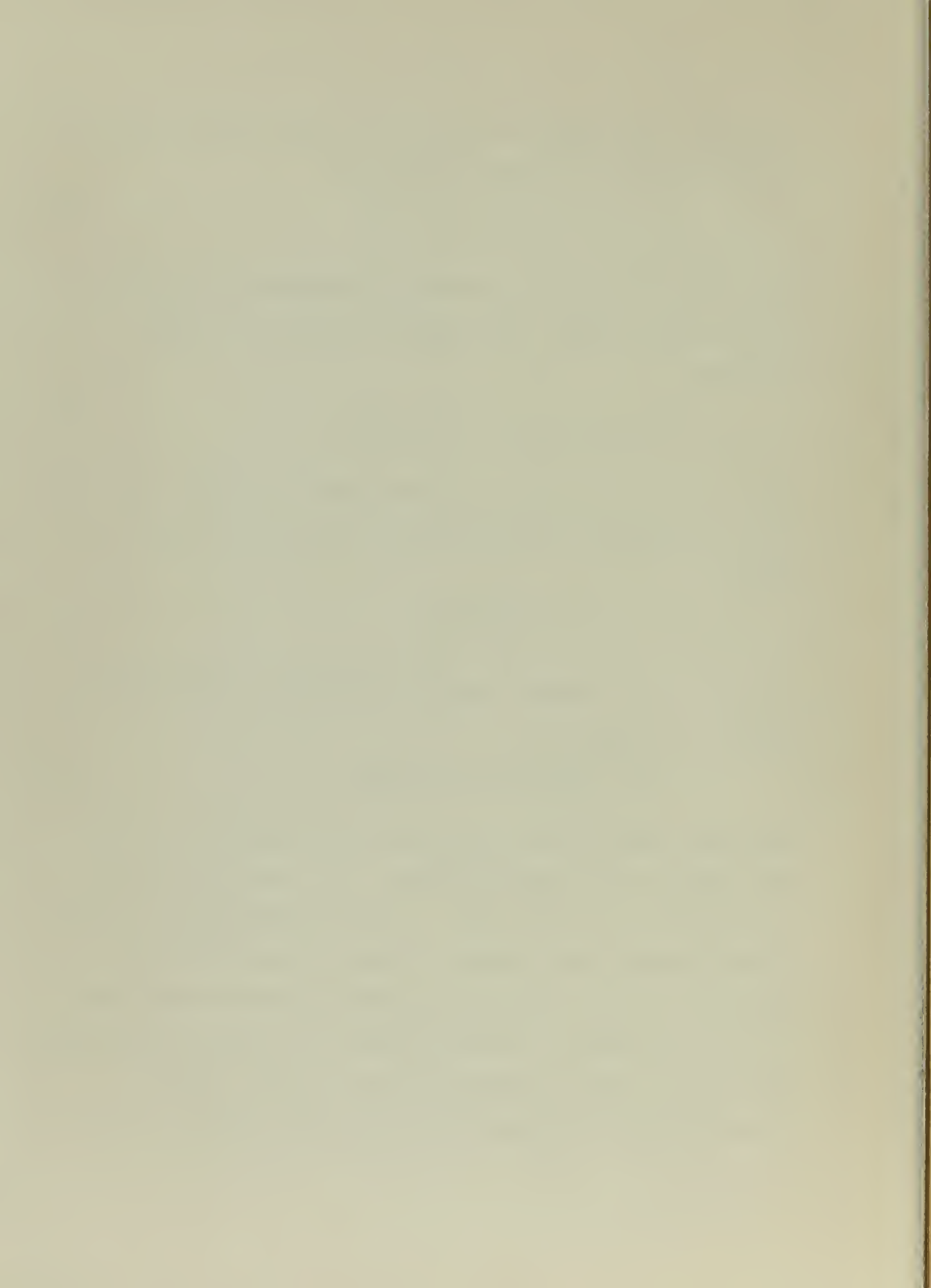
$$S = S'(N_L/N)[1 - \exp(-hc\omega_0/kT)],$$ (3)

where N is the total number of atoms per cm^3 per atmos, N_L is the number of atoms in the lower state per cm^3 per atmos. Here S' is given by

$$S' = \pi q^2 N f/m c^2,$$ (4)

where f is the "oscillator strength", which has been tabulated by Unsöld[1]. At equilibrium

$$N_L/N = (g_L/Q) \exp(-hc\omega_L/kT),$$ (5)

where g_L is the degeneracy of the lower state involved in the transition, and Q is the partition function. In this case g_L/Q is taken as n^2 and $\omega_L = R(1 - 1/n^2)$ where n is the principal quantum number of the lower state in the transition. In the present calculation the partition function is, for practical purposes, equal to the contribution from the ground state. For the temperatures and pressures considered here it may be shown, using the estimates of Urey[3], that this procedure does not introduce errors greater than about one percent. It

is now possible to write Eq. (3) as

$$S = S' n^2 [1 - \exp(-hc\omega_o/kT)] \exp [(1 - 1/n^2)(-Rhc/kT)].$$ (6)

To estimate the intensity width, $2|\omega_{\ell} - \omega_o|$, at half the value of $R_{max}(K)$, one uses the well known curves of growth (see, for example, Unsöld[1] or Penner and Kavanagh[2]). Here ω_{ℓ} is a wave number such that $R_{\omega}(K) = \frac{1}{2}R_{max}(K)$. The line shape parameter is given by

$$a = b_c (\ln 2)^{1/2}/b_D,$$ (7)

where the natural half width has been neglected compared to the collision half width, b_c . The Doppler half width, b_D , is given by

$$b_D = (2kT \ln 2 / m_u c^2)^{1/2} \omega_o.$$ (8)

An estimate of the collision half width is obtained from the formula of Weisskopf[4]:

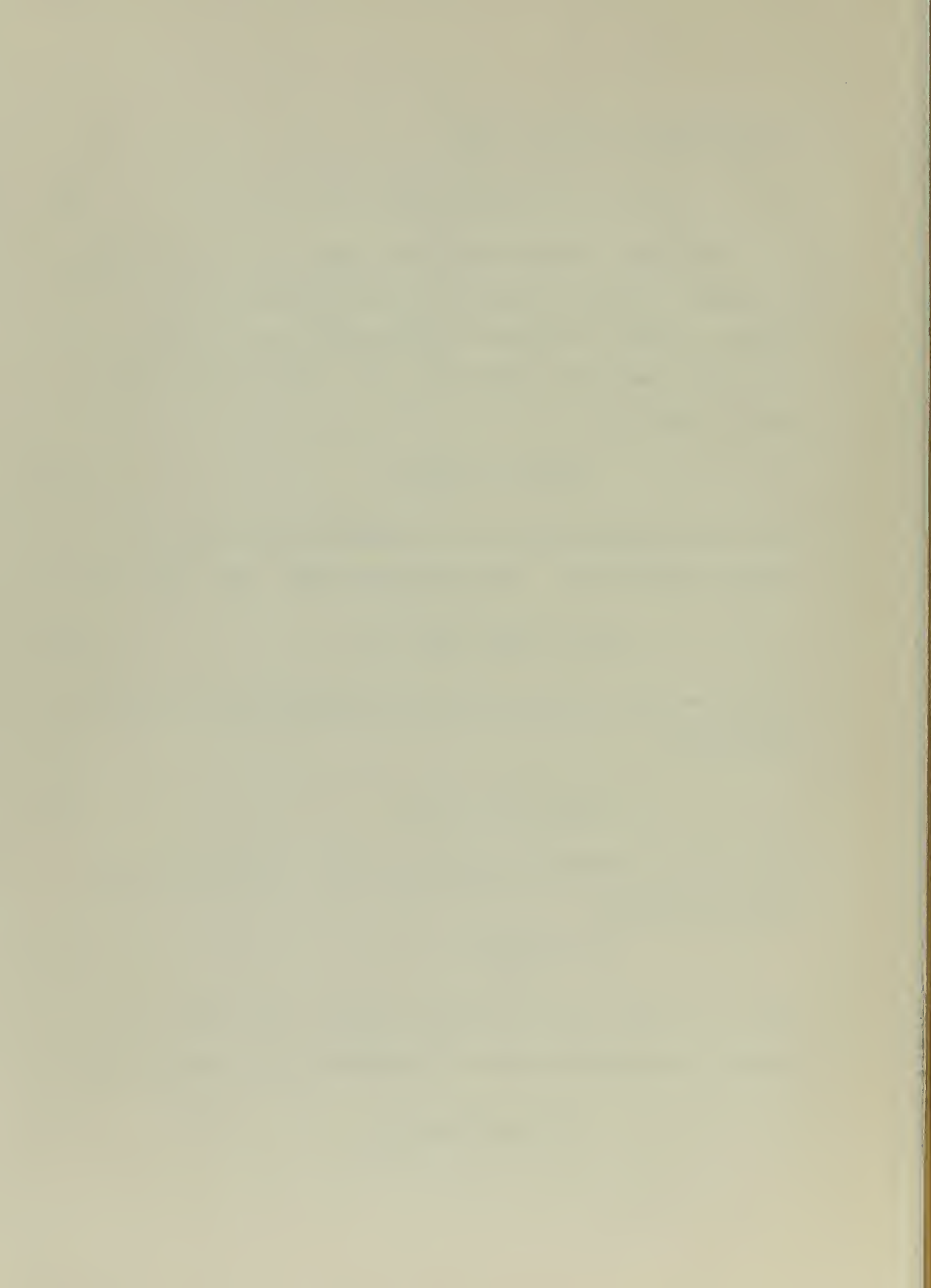$$b_c = q^2 n f / 2\pi m c^2 \omega_o,$$ (9)

where n is the number of molecules per cm^3. Combining Eqs. (4) and (9), one obtains

$$b_c = S' P_T / 2\pi^2 \omega_o,$$ (10)

where P_T is the pressure in atmos. Knowing a and $P'X$, it is possible to read from the curves of growth the value of the quantity S,

$$S = A(\ln 2)^{1/2}/2 R_{\omega}^o b_D,$$ (11)

where

$$A = 2|\omega_k - \omega_0| R_\omega^0.$$ (12)

Combining Eqs. (11) and (12), one obtains

$$|\omega_k - \omega_0| = 5 b_0/(\ln 2)^{1/2}.$$ (13)

If the Stark effect due to ionization is considered, P_ω^d may be taken as a first rough estimate, as $P_\omega^s + P_\omega^n$, where P_ω^s is the absorption coefficient due to ionization broadening alone, and P_ω^n is the absorption coefficient due to broadening without considering ionization. A relation for the absorption coefficient due to ionization broadening is given by

$$P_\omega^s = \frac{\alpha(\Delta\lambda) n^2 \exp(-hc\omega_L/kT) N_0}{R'T},$$ (14)

where N_0 is Avogardo's number, and $\alpha(\Delta\lambda)$ $(cm^2/atom)$ is the absorption coefficient per absorbing atom at a wave length $\Delta\lambda$ (A) from $1/\omega_0$. The relation for $\alpha(\Delta\lambda)$ is

$$\alpha(\Delta\lambda) = 4.21 C_n q^{3/2} N'/(\Delta\lambda)^{5/2}, \qquad *$$ (15)

where N', the number of protons per cm^3, may be determined from the Saha equation, and C_n has been tabulated by Aller[5] and

---

* For a more complete discussion of the Stark effect due to ionization see Ref. 5. Here broadening due to electrons is neglected. The electron effect has been discussed recently by B. Kivel, S. Bloom, and H. Margenau, Phys. Rev. 98, 495 (1955).
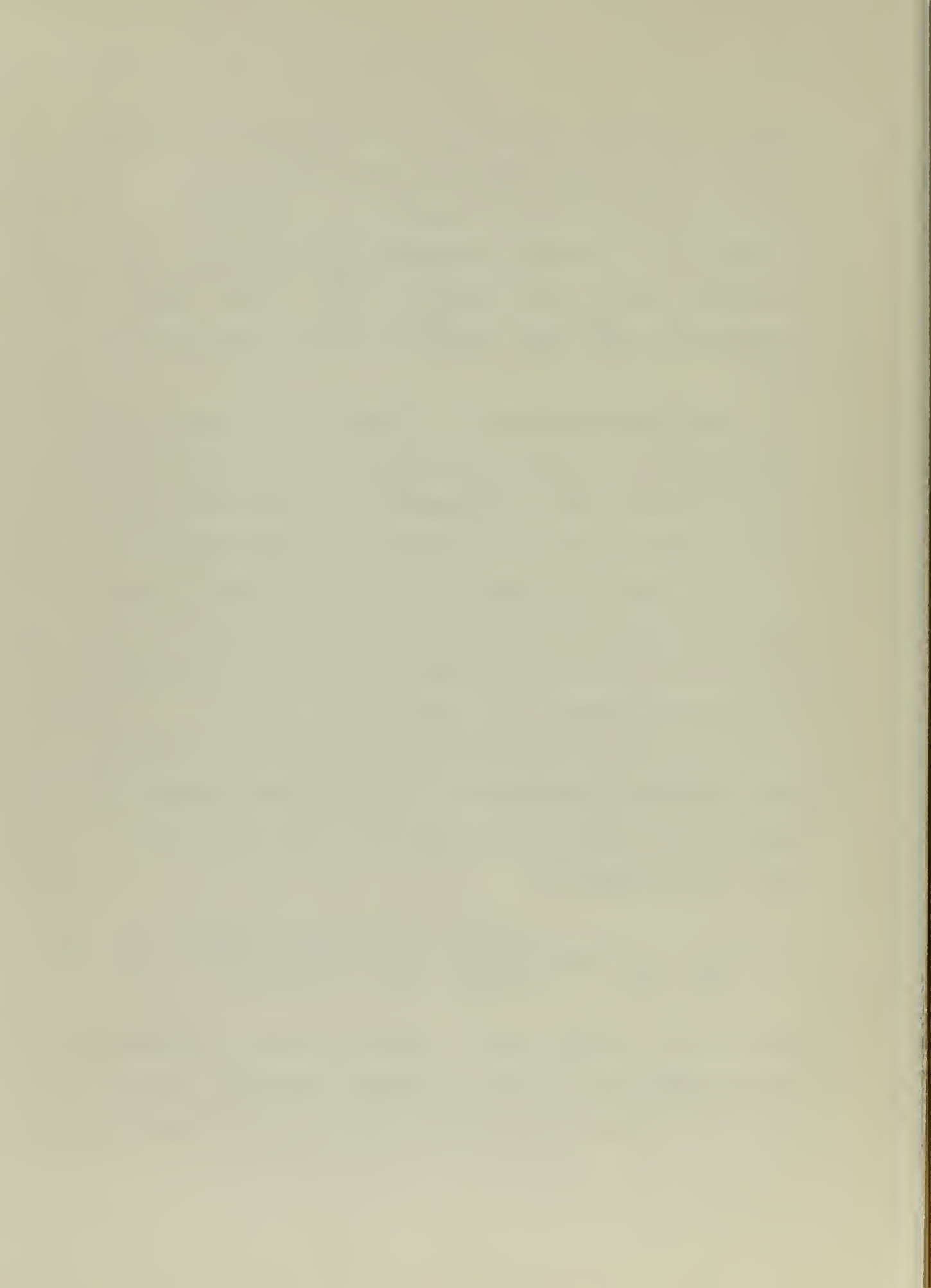
Unsöld[1]. Using Eqs. (14) and (15), a check of ionization broadening has been made at various temperatures and pressures using $H\alpha$ as an example. In all cases it was found that $[1 - exp(-P'_\omega X)] << 1$ at the value of ω_h previously determined without considering Stark broadening, so that it seems justifiable to take $P^n_\omega = P^a_\omega$ except perhaps for the Lyman lines, where the factor $exp(-hc\omega_L/kT)$ is unity.

The method described above to determine contributions to the emissivity due to discrete transitions does not apply in the case of the Lyman lines because they are too intense, and the blackbody curve along the intensity width of the lines varies appreciably in this area. At the temperatures considered here it is only necessary to determine modifications of the above method for Lyman α, since the succeeding Lyman lines give negligible contributions because of the small value of the blackbody radiancy, R°_ω, at large ω. When $(\omega - \omega_0)$ is, for example, of such magnitude that it does not overlap an adjoining line, an expression for the discrete pressure broadening absorption coefficient, P^n_ω, has been given by Born[2]. For large values of ξ/a, Born's relation is

$$\frac{P^n_\omega}{P'} = \left(\frac{1}{a\sqrt{\pi}} \frac{1}{1+(\xi/a)^2}\right)\left\{1 - \frac{1}{2}\left(\frac{1}{a}\right)^2 \frac{1 - \left(\frac{3}{2}\right)(\xi/a)^2}{[1+(\xi/a)^2]^2} + \frac{3}{4}\left(\frac{1}{a}\right)^4 \frac{1 - \left(\frac{5}{2}\right)(\xi/a)^2 + \left(\frac{5}{4}\right)(\xi/a)^4}{[1+(\xi/a)^2]^4} + \cdots\right\}, \quad (16)$$

where $\xi = [(\omega - \omega_0)/b_0](\ln 2)^{1/2}$. When $(\omega - \omega_0)$ is, for example, of such magnitude that it overlaps an adjoining line, Born's method for pressure broadening and the treatment described above for the Stark
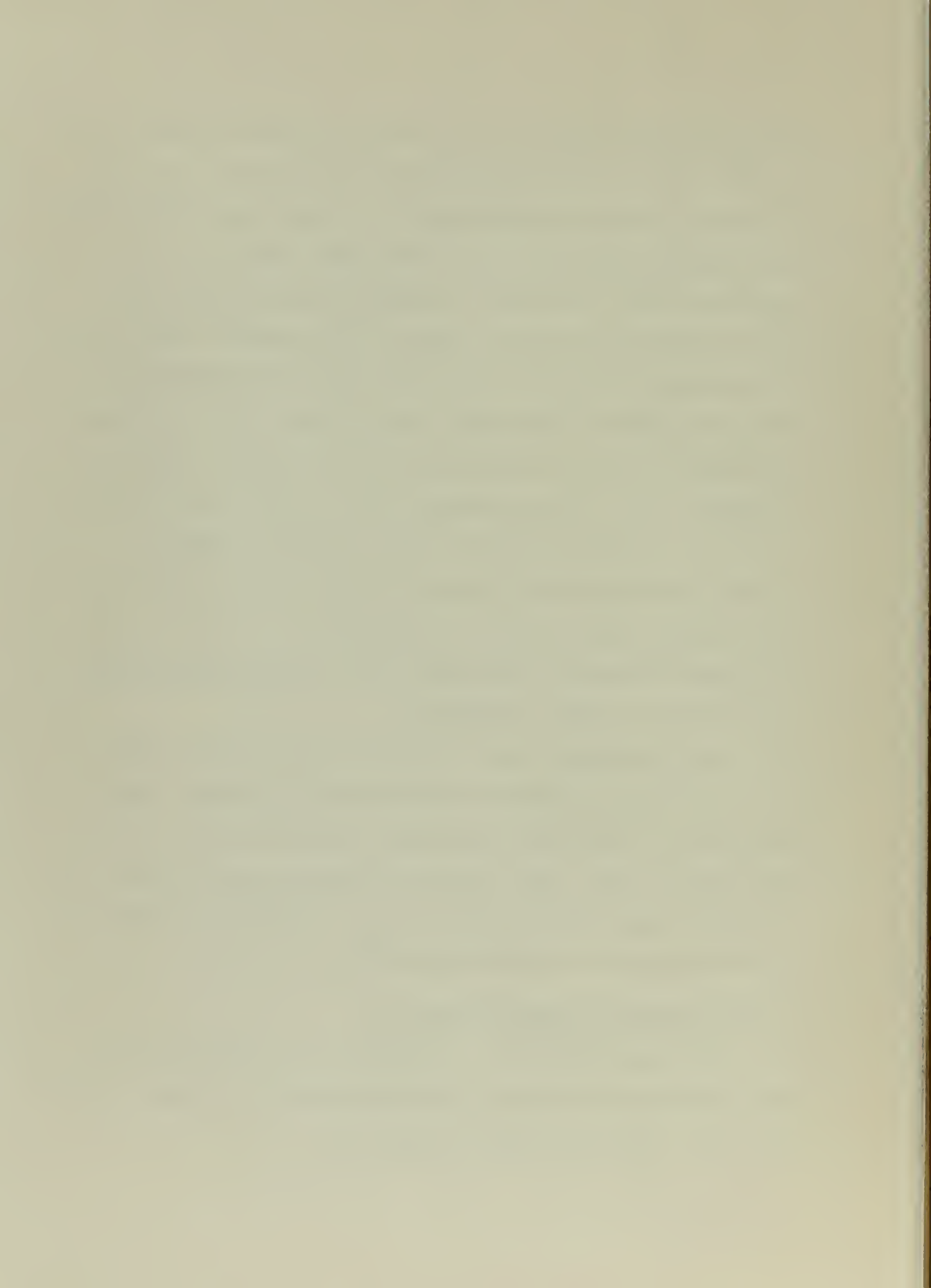
effect do not apply because one can no longer consider the contributions as resulting from "small" perturbations of well defined energy states. The problem of the very broad Lyman α line has caused difficulty in related astrophysical applications, and an exact treatment is not feasible at present. Therefore, a reasonable cut-off point has been chosen beyond which the above treatment is not justifiable. The cut-off point to the left of the line is taken arbitrarily as one half the distance between the Lyman α and Lyman β line centers. The cut-off point to the right of the line is unimportant since the blackbody contribution is negligibly small. The application of Eqs. (14), (15), and (16) to the Lyman lines results effectively in adding a small contribution of blackbody radiation from the left cut-off point to $\omega = \infty$. It is felt that the neglect of the Lyman α contribution from $\omega = 0$ to the left cut-off point does not give appreciable error, but this approximation may well deserve further investigation.

The contributions due to the higher series, Brackett, Pfund, etc., have not been considered in the present computations. These series will give appreciable contributions only at much lower temperatures than were used. Even if these contributions were blackbody from the left of the first Paschen line to $\omega = 0$, the emissivity would in no case be increased by more than about 1 $^o/o$.

B. Determination of Optical Density X

The optical density, X, is defined as $\rho_H \ell$ where ρ_H is the partial pressure of the hydrogen atoms (atmos) and ℓ is the geometric depth (cm). The partial pressure is given as

$$\rho_H = (2x/1+x)P_T, \tag{17}$$

where x is the degree of dissociation of hydrogen molecules and P_T is the total pressure. The degree of dissociation, x, may be determined from
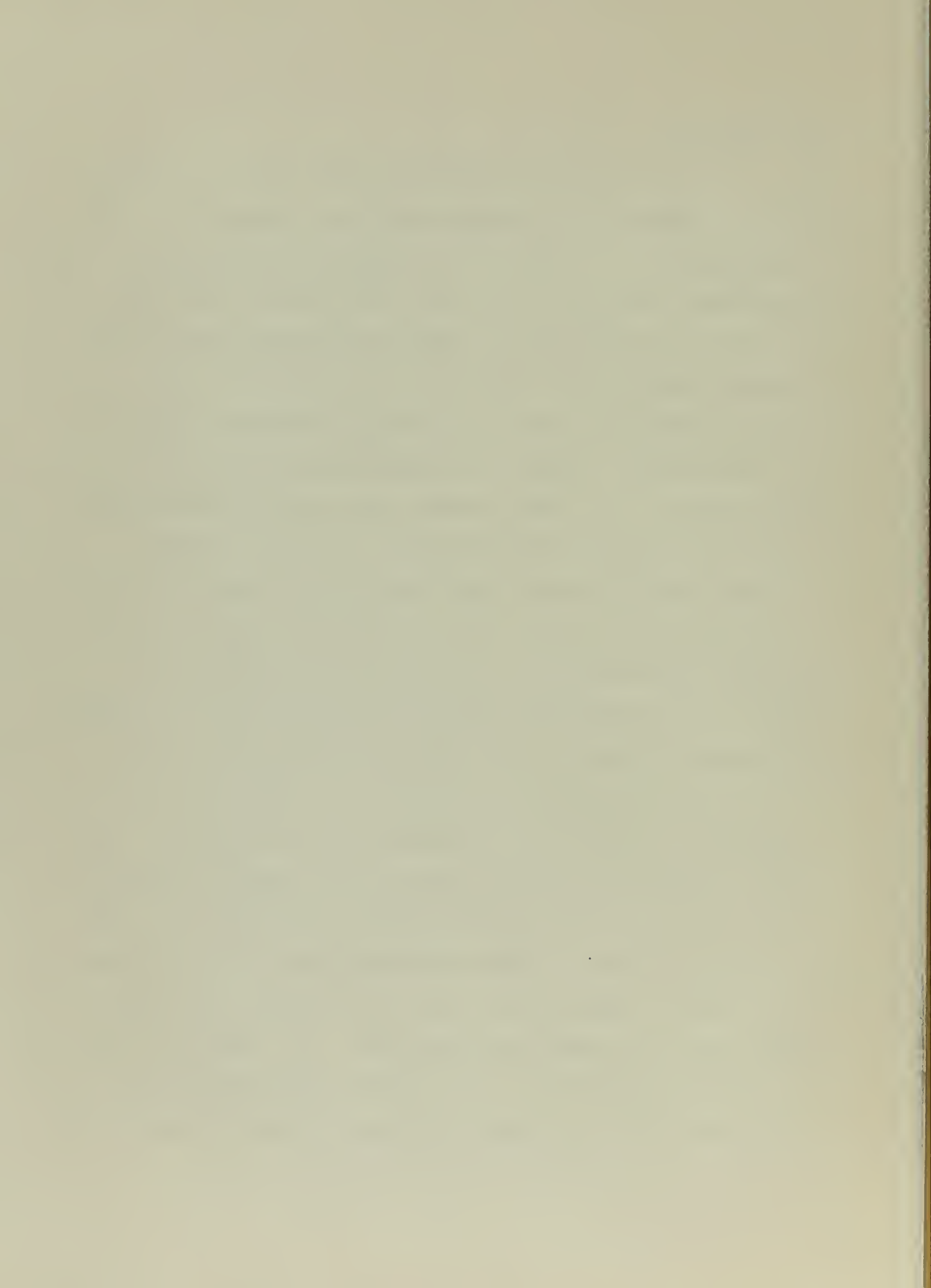
$$K_P = (4 x^2/1 - x^2)P_T, \tag{18}$$

where K_P is the equilibrium constant for the dissociation of molecular hydrogen. Good estimates of K_P can be obtained by extrapolating data given in the National Bureau of Standards Tables[6].

Values of x and ρ_H are listed in Table I. From this table it is seen that hydrogen atoms may be expected to contribute significantly to the total emissivity. In a more exact treatment it would be necessary to consider the contributions of species other than hydrogen atoms which are present in relatively small amounts at the temperatures and pressures considered in the present investigations.
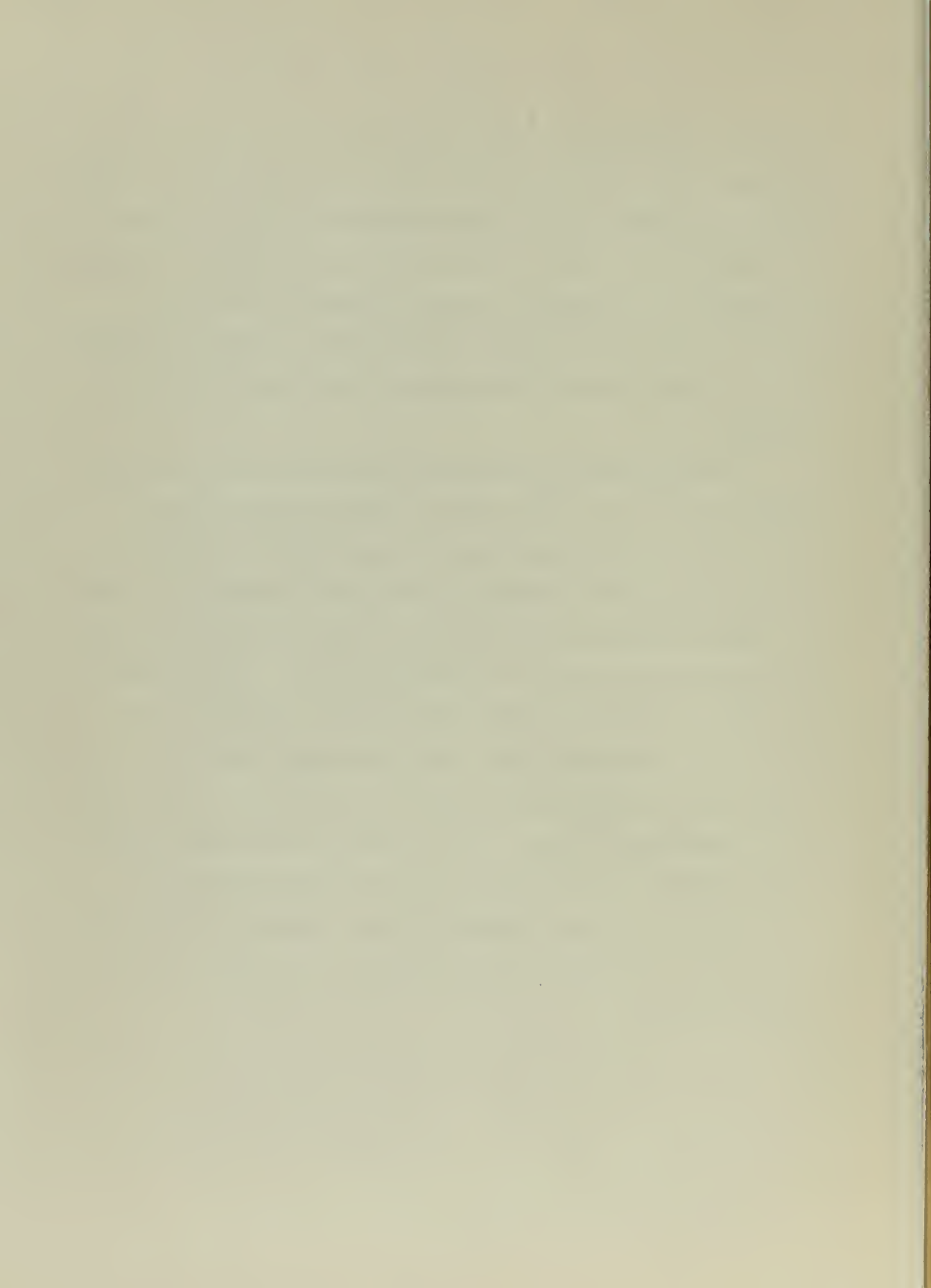
III. RESULTS

By use of the above procedures the total emissivity of hydrogen atoms in equilibrium with hydrogen molecules at various temperatures and pressures has been computed. For most of the computations a characteristic geometrical depth of 50 cm has been used, and Figs. 1 to 7 refer to that depth, as does the following discussion except where explicitly noted otherwise. In the ranges of temperatures and pressures chosen, the emissivity varies significantly with changes in the state variables. Typical plots used to determine the emissivity are shown in Figs. 1 to 5, where the outer curve represents the blackbody curve, the cross-hatched area represents contributions from the continuous spectrum, and the solid area represents added contributions from the discrete transitions. The discontinuities in the continuous spectrum portions of Figs. 1 to 5 correspond to the onsets of the various continua; the Pfund continuum begins to contribute at $\omega = 4380$, the Brackett continuum at $\omega = 6850$, the Paschen continuum at $\omega = 12190$, and the Balmer continuum at $\omega = 27400$. It is not necessary to consider the Lyman continuum for the temperatures used here. As seen from the figures, the continuous spectrum contributions to the emissivity increase as the temperature increases. The significant lines are located as follows: Paschen series, $\omega_0 = 5330$, 7790, 9130, 9940, and 10480; Balmer series, $\omega_0 = 15220$, 20580, 23050, 24400, 25150, and 25750; and Lyman series, $\omega_0 = 82200$. As may also be seen from the figures, the intensity width increases as the temperature increases, and hence discrete transition contributions also

increase. In general, the continuous spectrum gives the major contribution to the emissivity at high temperatures ($T \gtrsim 9200^{\circ}$K), and the discrete transitions give the major contribution at low temperatures ($T \lesssim 9200^{\circ}$K). In a similar manner it may be shown that for a constant temperature the emissivity increases with pressure because the number density of emitters increases (fixed l, X increasing) linearly with pressure; furthermore, the lines are broadened as the pressure is raised.

The data listed in Table II are obtained from such plots as are shown in Figs. 1 to 5. These data are shown in graphical form in Figs. 6 and 7. From these figures it is seen that the emissivity approaches unity ($\epsilon \gtrsim 0.95$) for temperatures of the order of $12,500^{\circ}$K and higher, with pressures of the order of 100 atmos and higher, while for temperatures of the order of 9500°K and lower, with pressures of the order of 10 atmos and lower, the emissivity approaches zero ($\epsilon \lesssim 0.05$). The graph in Fig. 8 shows the change in the total emissivity as a function of geometrical depth for constant temperature ($T = 12,600^{\circ}$K) and pressure ($P_T = 20$ atmos). If either the temperature or pressure is decreased, the emissivity decreases and the ϵ vs l curve lies under the curve shown. Similarly, if either the temperature or pressure is increased, the ϵ vs l curve lies above the curve shown.

REFERENCES

(1)   A. Unsöld, Physik der Sternatmospharen, J. Springer, Berlin, 1938.

(2)   S. S. Penner and R. W. Kavanagh, J. Opt. Soc. Am. 43, 385, 1953.

(3)   H. C. Urey, Astrophys. J. 59, 1, 1924. See also E. Fermi, Z. Physik 26, 54, 1924 and R. V. Meghreblian, Ph. D. Thesis, California Institute of Technology, 1953.

(4)   H. Margenau and W. W. Watson, Revs. Modern Phys. 8, 41, 1936.

(5)   L. H. Aller, The Atmospheres of the Sun and Stars, Ronald Press Co., New York, 1953, p. 311.

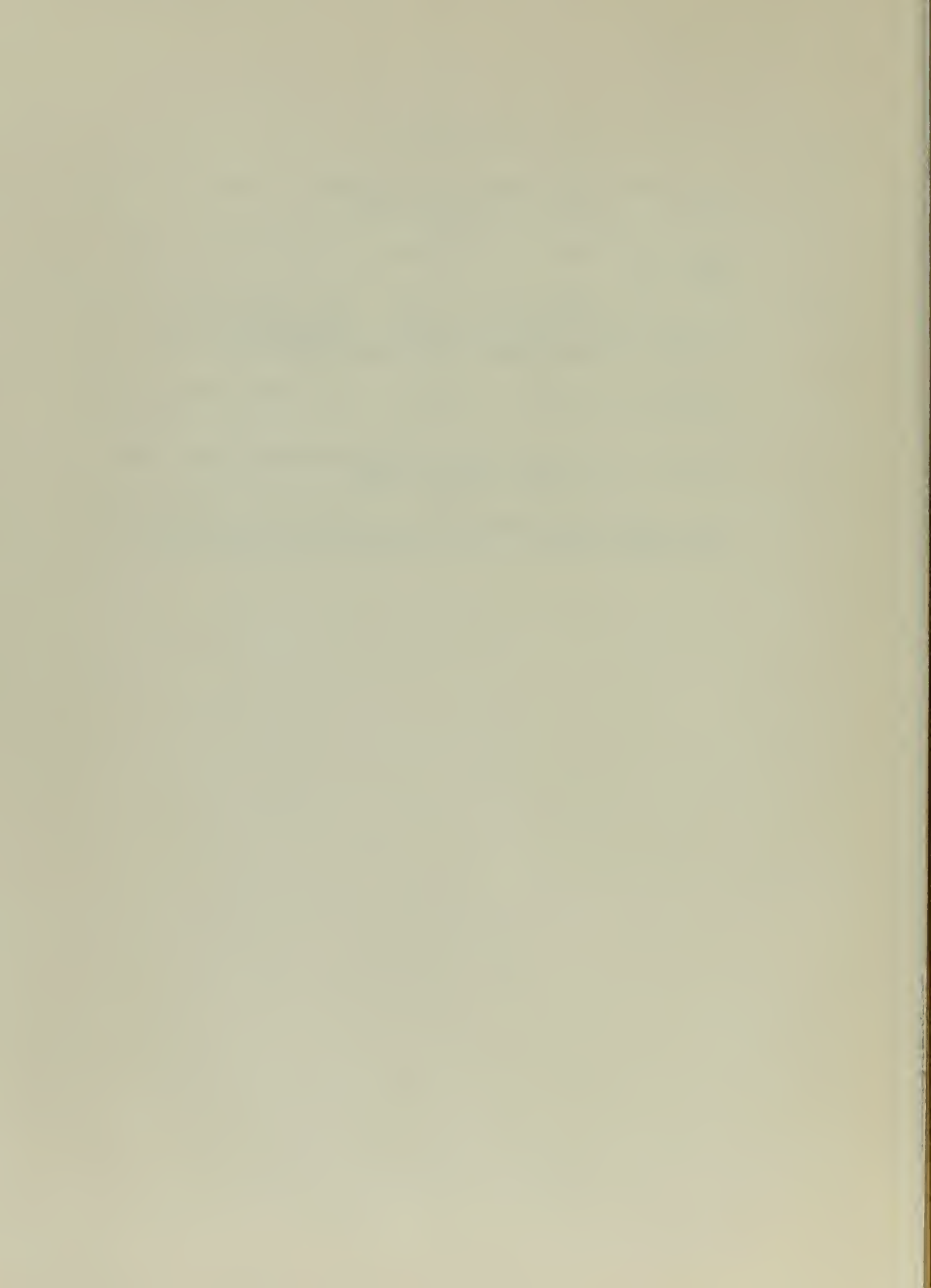(6)   NBS, Tables of Selected Values of Chemical Thermodynamic Properties, Series I, Vol. I, March 1947 to June 1949.

TABLE I. FRACTION OF H_2 DISSOCIATED (χ) AND PARTIAL PRESSURE IN ATMOSPHERES OF ATOMIC HYDROGEN (P_H) AT VARIOUS TEMPERATURES AND TOTAL PRESSURES.

P_T	8400°		9200°		10080°		11300°		12600°	
	χ	P_H	χ	P_H	χ	P_H	χ	P_H	χ	P_H
50	0.976	49.5								
100	0.953	97.5	0.974	98.6	0.984	99.0				
150	0.932	145	0.961	147	0.977	148	0.986	149		
200	0.914	191	0.950	195	0.968	197	0.983	198	0.990	199

TABLE II. EMISSIVITY OF ATOMIC HYDROGEN AS A FUNCTION
OF TEMPERATURE AND TOTAL PRESSURE
(l = 50 cm).

	8400°K	9200°K	10080°K	11300°K	12600°K
P_T (atmos)	ϵ	ϵ	ϵ	ϵ	ϵ
10	.014	.037	.085	.26	.48
20	.030	.071	.16	.35	.66
40	.063	.14	.28	.57	.83
70	.11	.24	.43	.74	.92
100	.15	.32	.55	.82	.96
150	.22	.44	.69	.89	
200	.30	.54	.75		

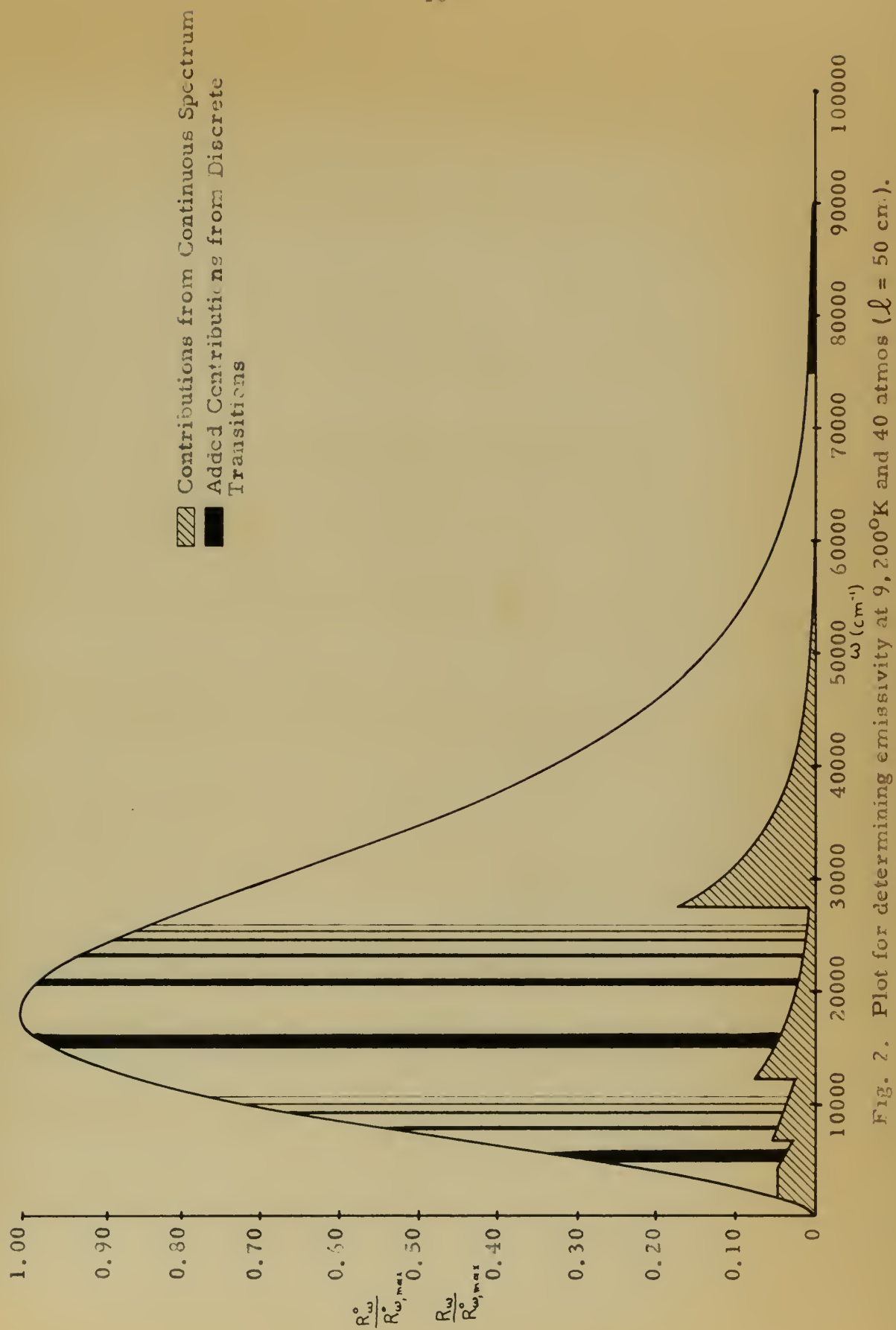Fig. 1. Plot for determining emissivity at 8400°K and 40 atmos ($\ell = 50$ cm).

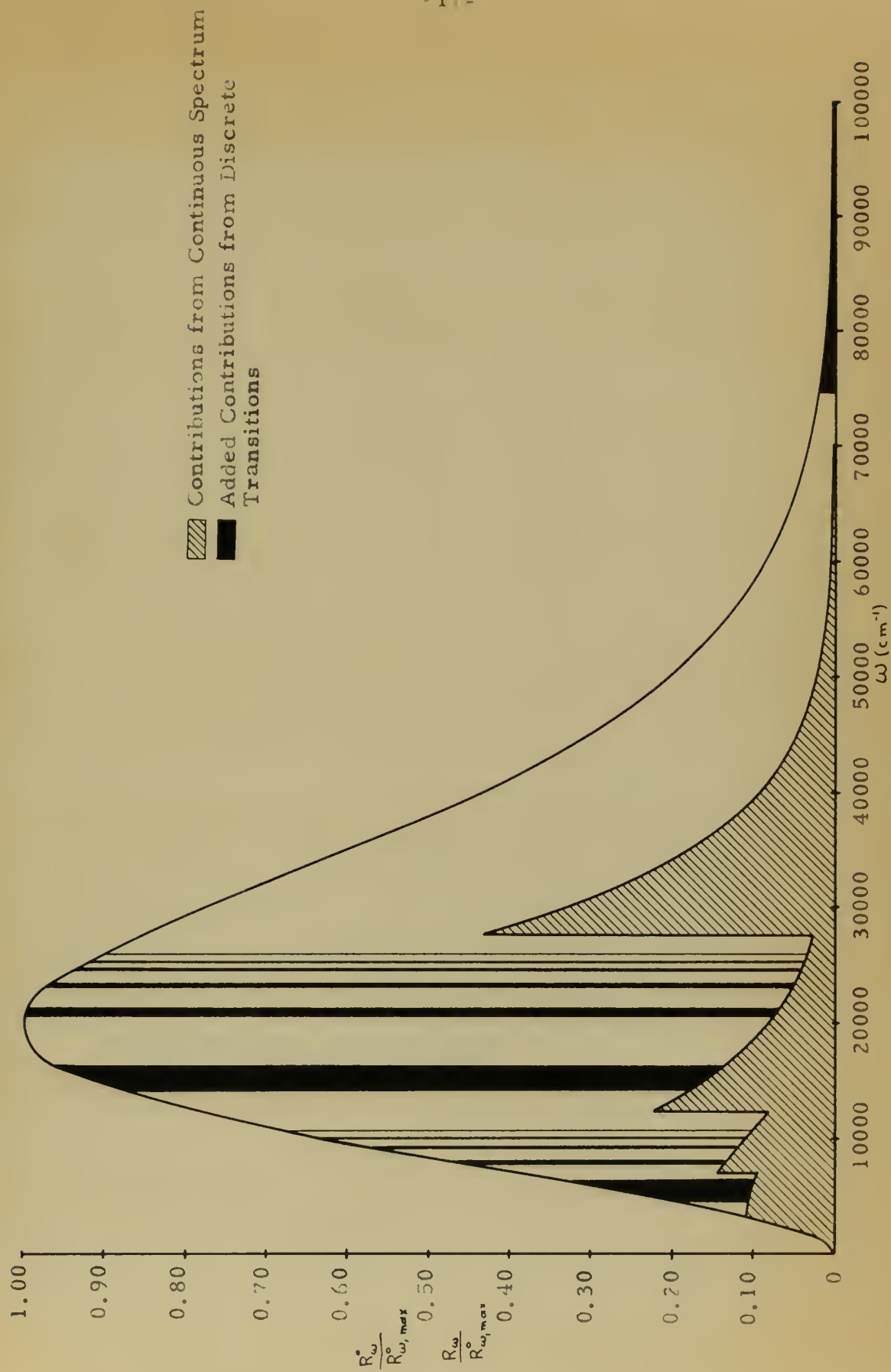Fig. 2. Plot for determining emissivity at 9,200°K and 40 atmos (ℓ = 50 cm.).

Fig. 3. Plot for determining emissivity at 10,080°K and 40 atmos (ℓ = 50 cm).
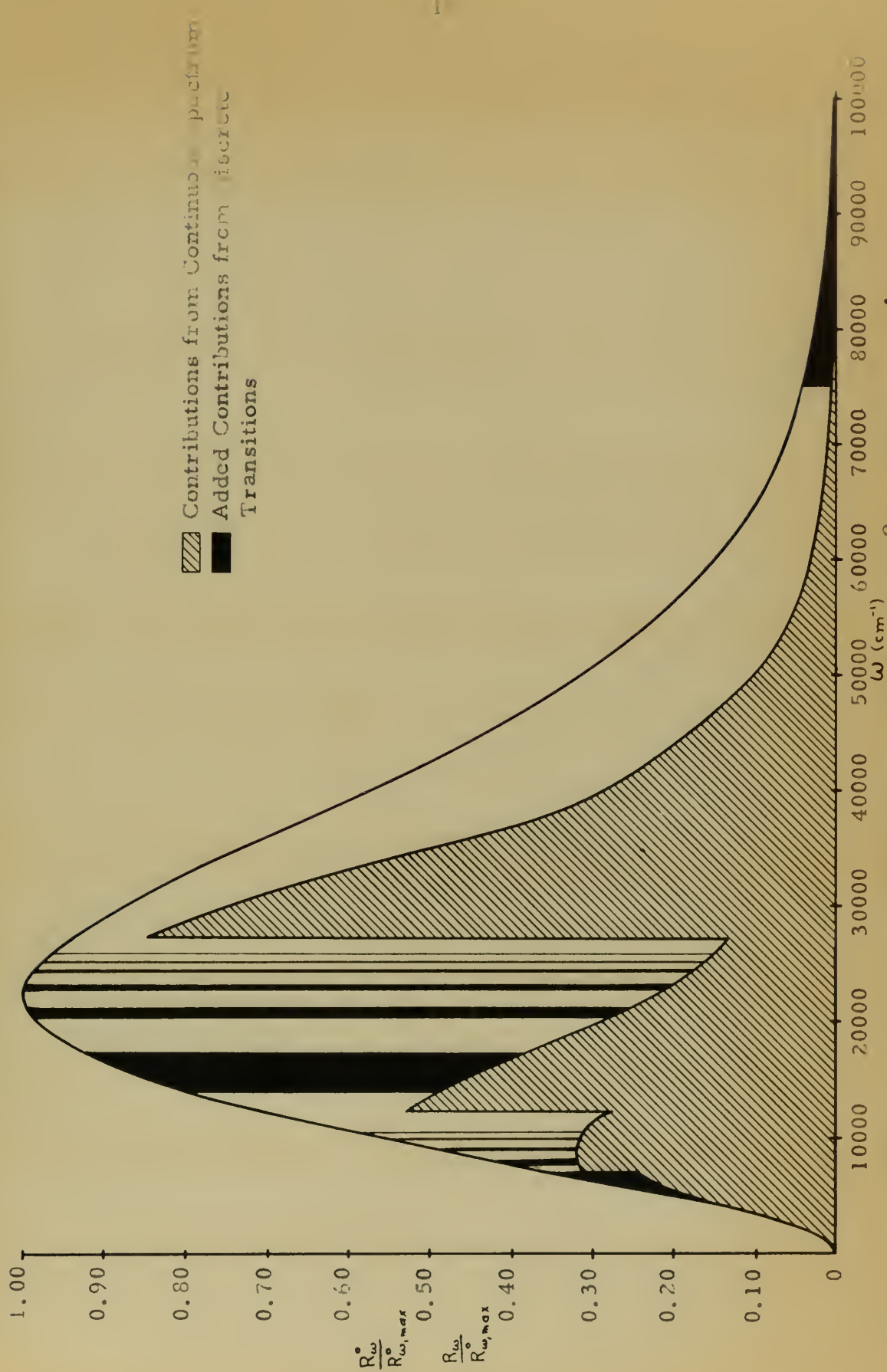
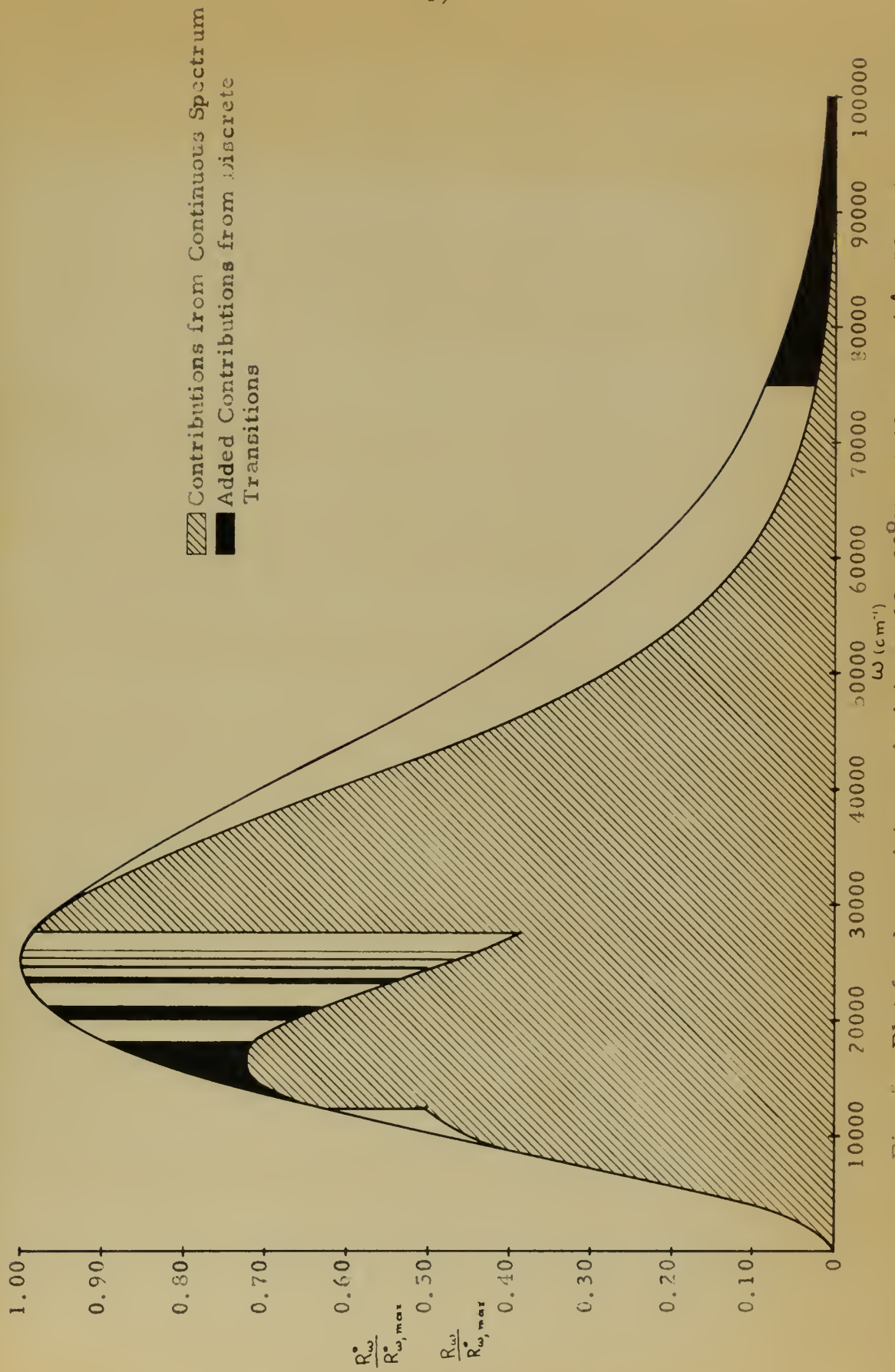Fig. 4. Plot for determining emissivity at 11,300°K and 40 atmos ($\ell = 50$ cm).
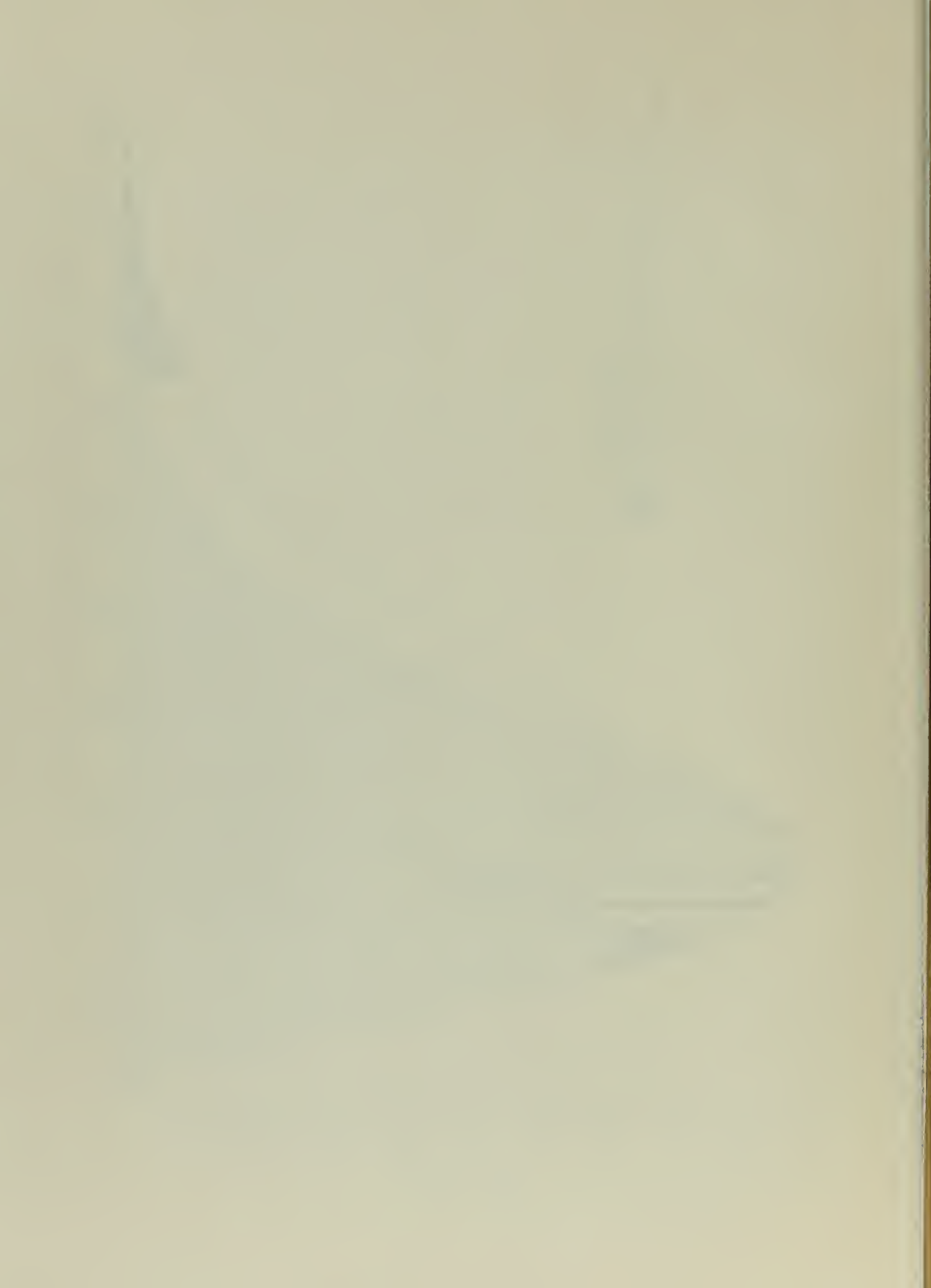
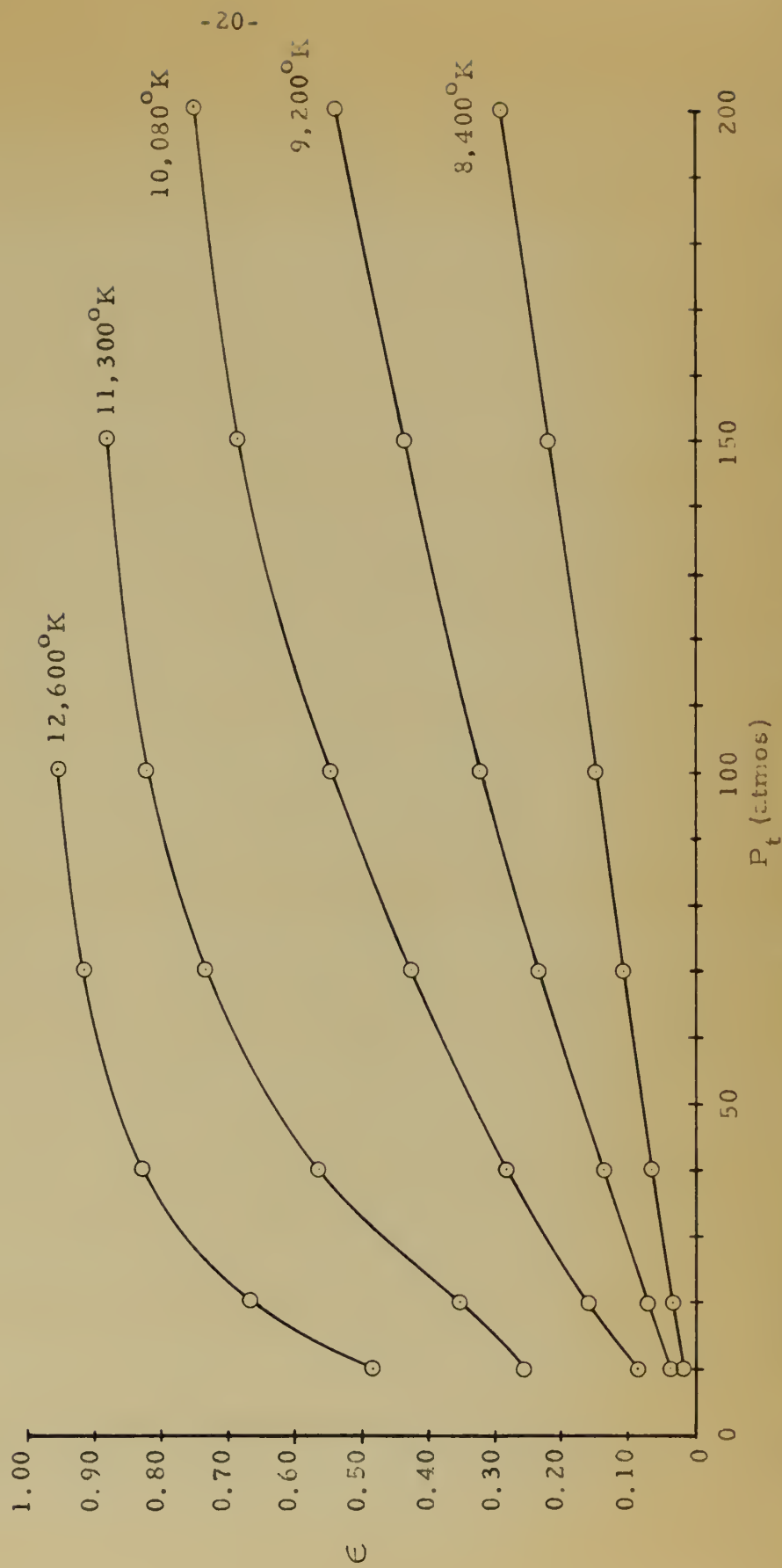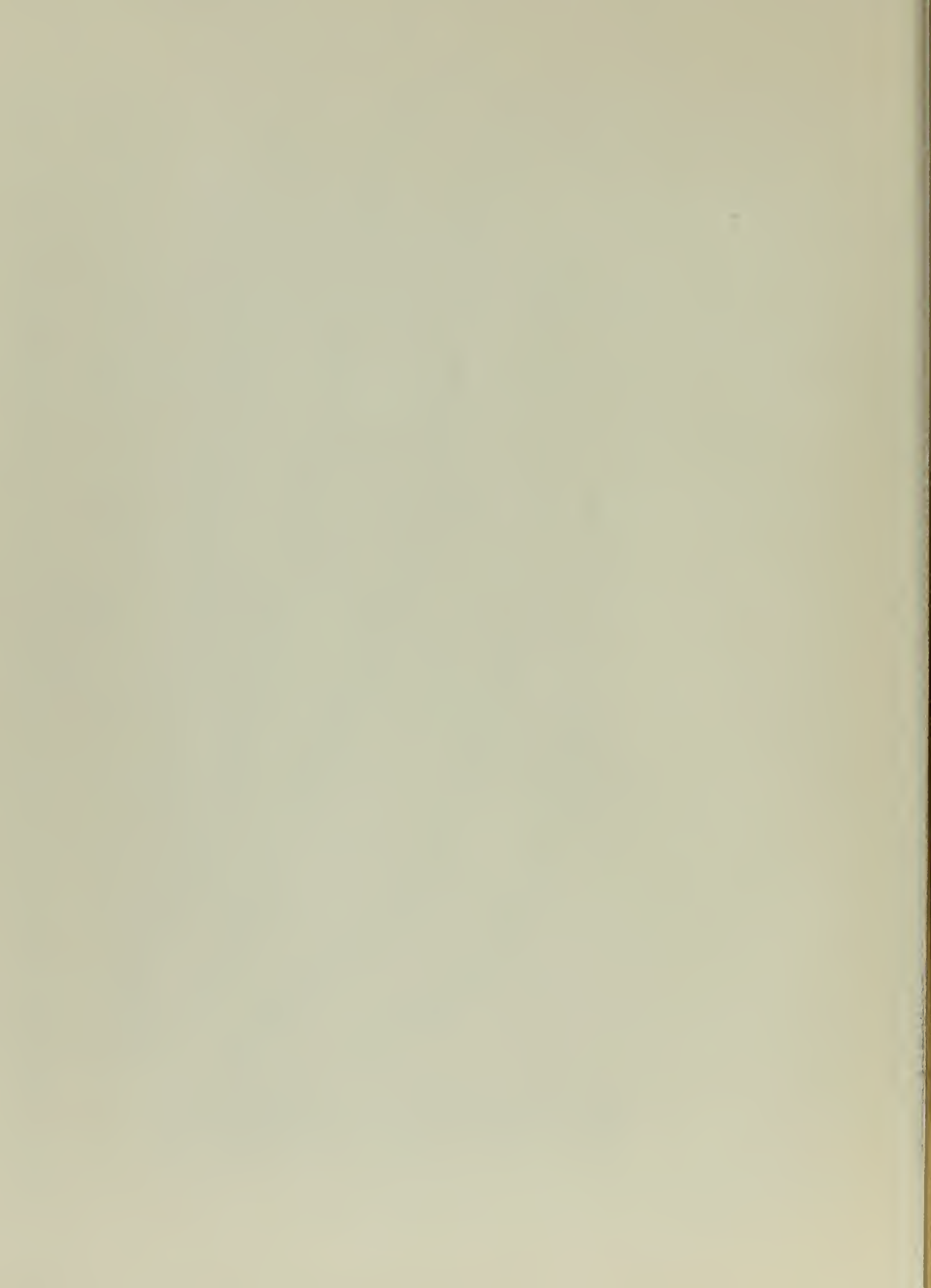Fig. 5. Plot for determining emissivity at 12,600°K and 40 atmos (ℓ = 50 cm).

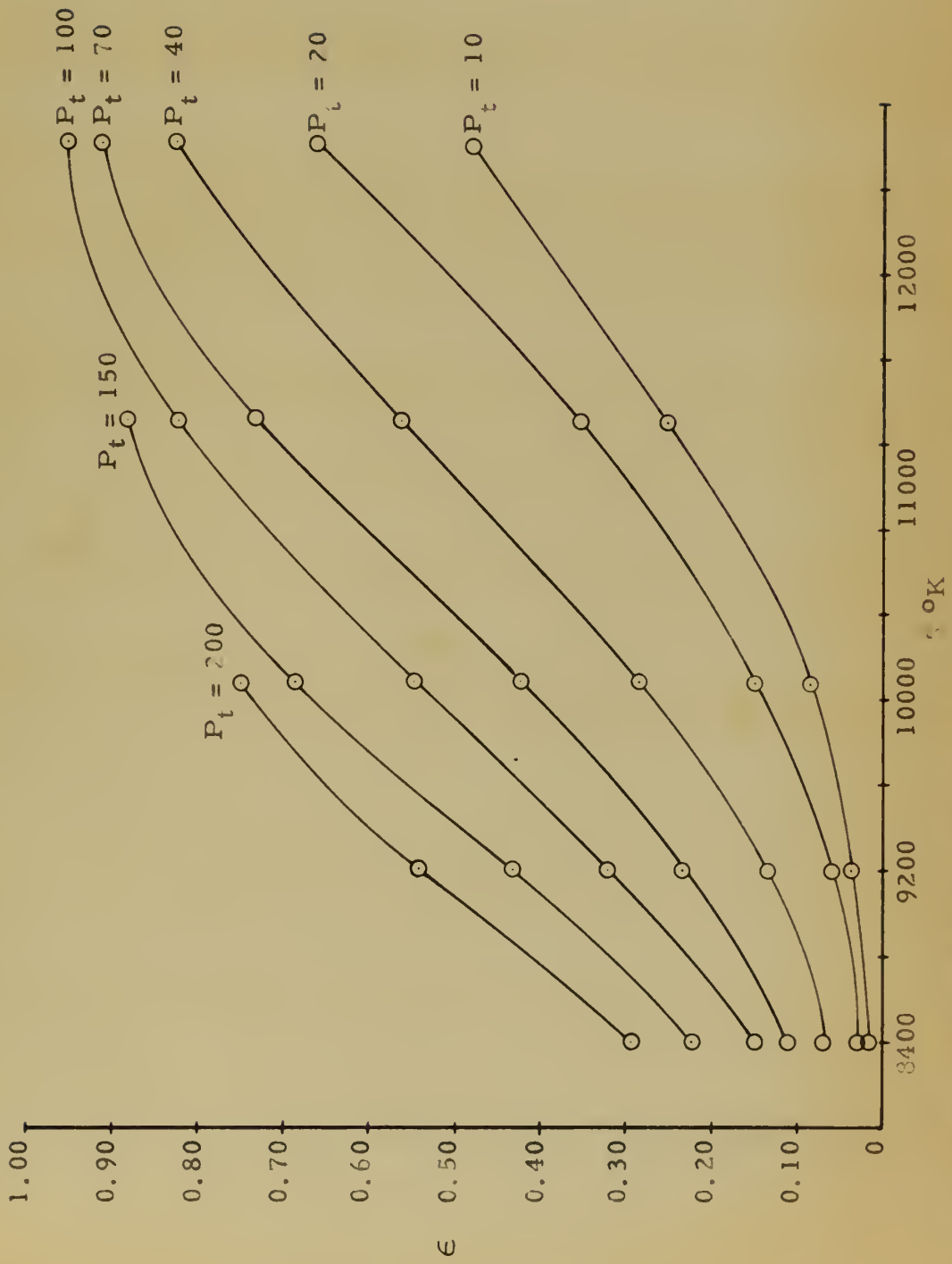Fig. 6. Emissivity of hydrogen atoms at various temperatures as a function of total pressure ($\ell = 50$ cm).

Fig. 7. Emissivity of hydrogen atoms at various total pressures as a function of temperature ($\ell = 50$ cm).
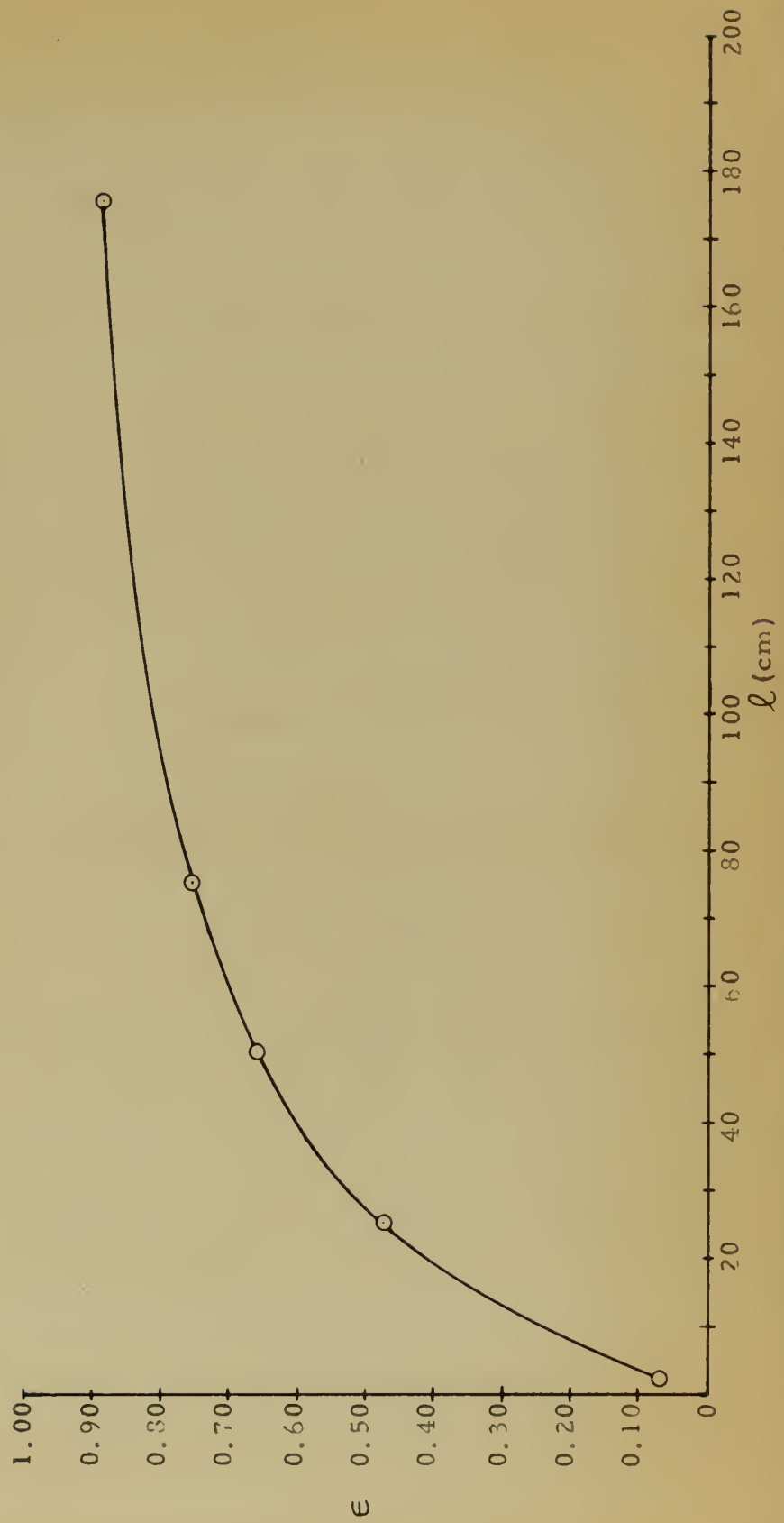
Fig. 8. Emissivity of hydrogen atoms as a function of geometrical depth ($T = 12,600°K$, $P_t = 20$ atmos).

APPENDIX

A. Sample Calculation

A detailed computation is presented here in order to show an application of the previously described procedure more clearly. This specific calculation is for the emissivity at 10080°K and $P_T = 40$ atmos with $l = 50$ cm. The values used for the various constants are as follows:

$$c = 2.9979 \times 10^{10} \text{ cm/sec}$$

$$h = 6.6238 \times 10^{-27} \text{ erg-sec}$$

$$k = 1.3803 \times 10^{-16} \text{ erg/}^\circ\text{K}$$

$$\sigma = 5.6699 \times 10^{-5} \text{ erg/cm}^2\text{-sec-}^\circ\text{K}$$

$$q = 4.8022 \times 10^{-10} \text{ esu}$$
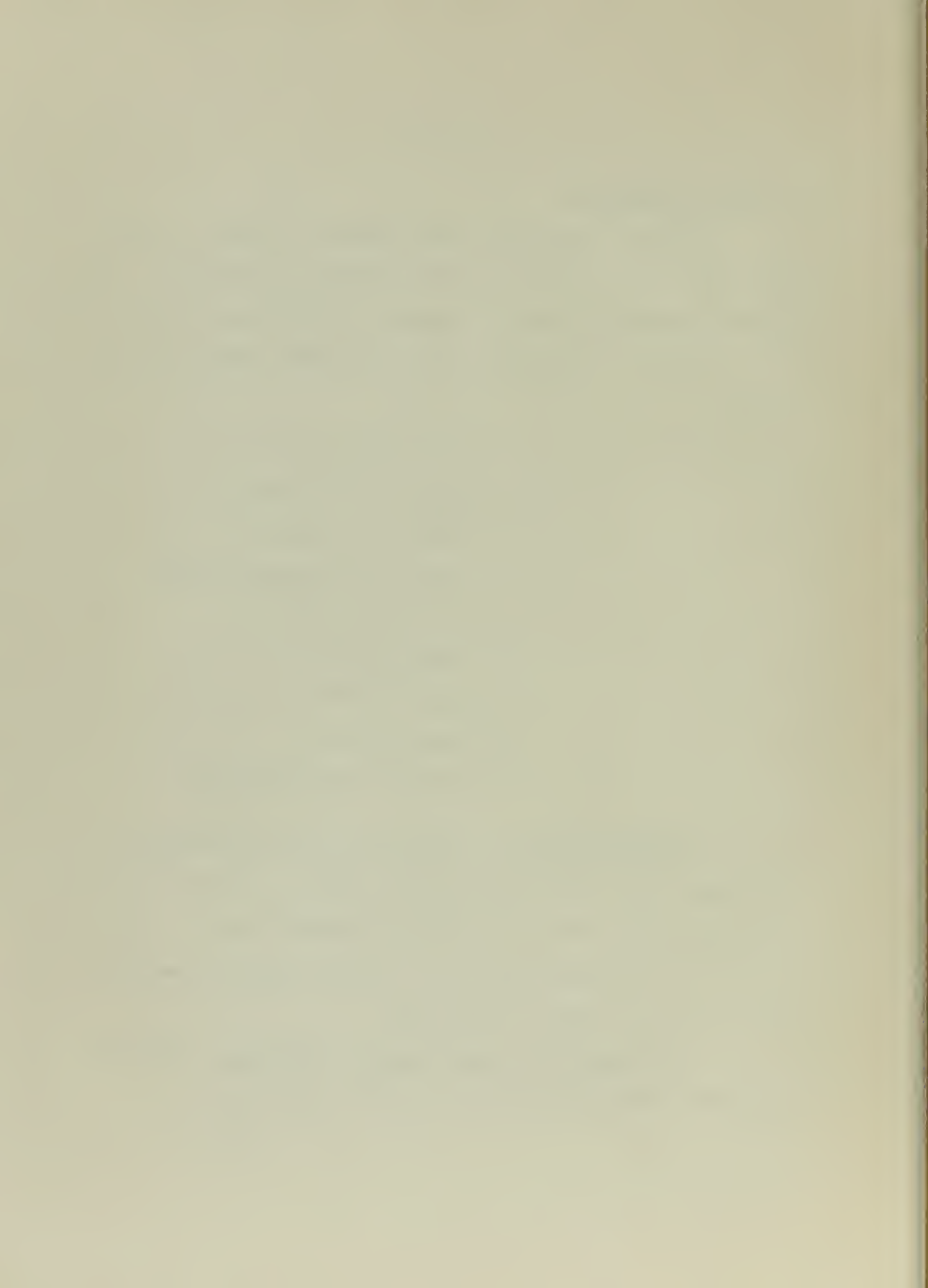
$$m = 9.1072 \times 10^{-28} \text{ g}$$

$$m_H = 1.6819 \times 10^{-24} \text{ g}$$

$$R = 1.0968 \times 10^5 \text{ cm}^{-1}$$

$$R' = 82.06 \text{ cm}^3\text{-atmos/mole-}^\circ\text{K}$$

1. Blackbody Curves. The blackbody curves are plotted using the relation $R_\omega^\circ = 2\pi h c^2 \omega^3 / \left[\exp(hc\omega/kT) - 1 \right]$. For $T = 10080^\circ$K this becomes $R_\omega^\circ = 3.74 \times 10^{-5} \omega^3 / \left[\exp(1.427 \times 10^{-4} \omega) - 1 \right]$. Values of R_ω° vs ω are shown in Table A-I. The area under the blackbody curve, σT^4, is 5.85×10^{11} erg/cm^2-sec.

2. Contributions from the Continuous Spectrum. The mass absorption coefficient [Eq. (1)] at 10080°K is given by

$$\chi'_\nu = (9.62 \times 10^{-14})[1 - \exp(-1.427 \times 10^{-2}\omega)]\, G/\omega^3, \qquad (\text{A-1})$$

where $G = \sum_{u_n < u}^{u_4} e^{u_n}/n^3 + e^{u_s}/2\,u_1$. Values of G obtained from Unsöld[1]
are as follows:*

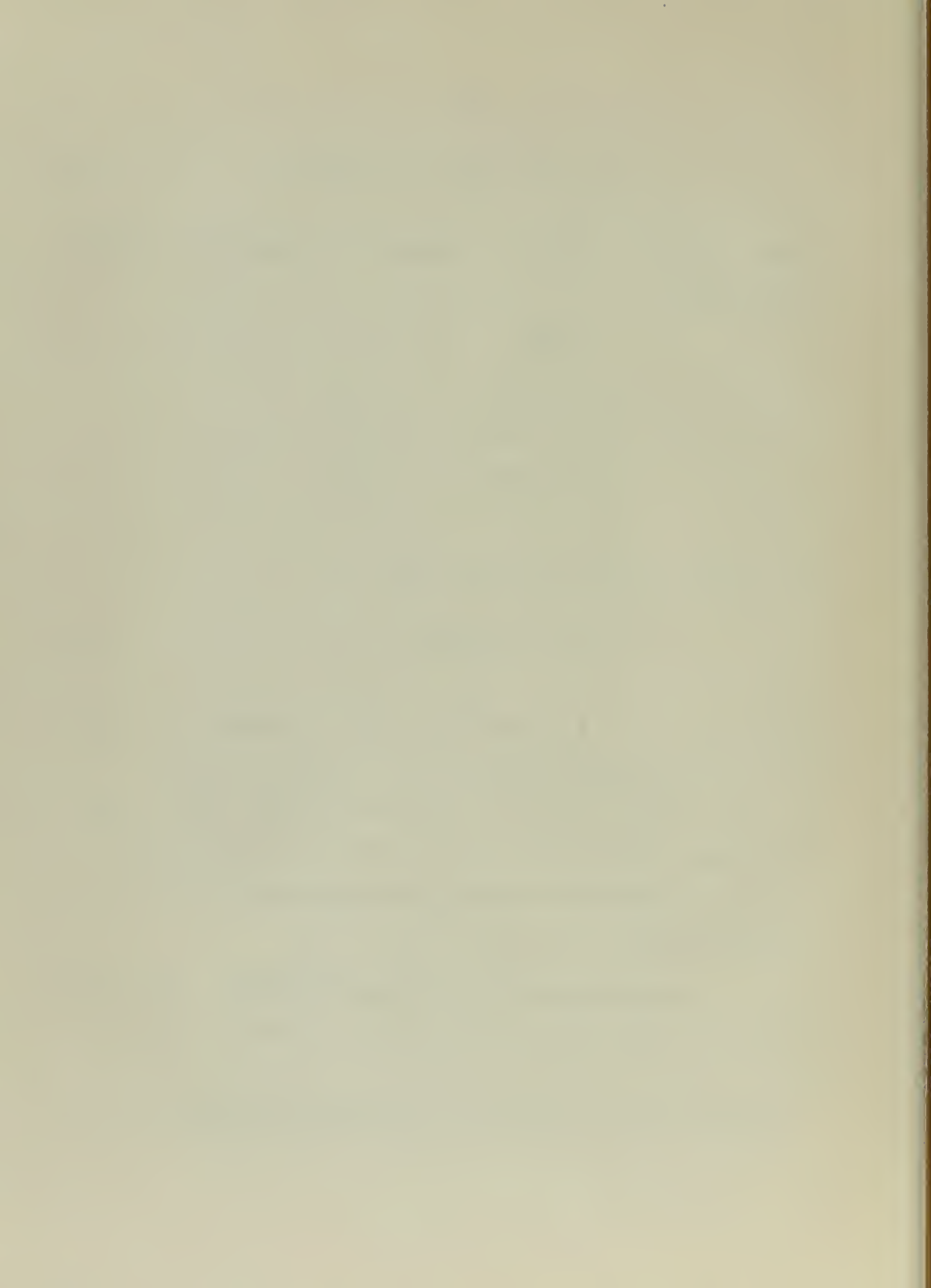| $\omega/10^3$	G
4.38 to 6.85	0.0596
6.85 to 12.19	0.101
12.19 to 27.4	0.309
27.4 to 109.7	6.43

The spectral absorption coefficient, P_ω^c , is

$$P_\omega^c = \chi'_\nu (1.008)/R'T, \qquad (\text{A-2})$$

from which $P_\omega^c = 1.216 \times 10^{-6}\, \chi'_\nu$. The optical density, $X = \rho_H \ell$,
is 1998 cm-atmos for this case ($\rho_H = 39.95$ atmos). The term
$[1 - \exp(- P_\omega^c X)]$ can now be determined, and hence R_ω^c can also
be obtained. Table A-II lists values of P_ω^c and R_ω^c for various ω .
The area of contributions from the continuous spectrum is found by
graphical methods to be 1.118×10^{11} erg/cm^2-sec.

3. Contributions from the Discrete Transitions. To calculate
p' as given in Eq. (2), it is first necessary to compute S' [Eq. (4)]

---

* Unsöld does not list values of G for 9200°K and 11300°K; however,
these can easily be calculated as indicated by the formula for G .

and S [Eq. (6)]. The value of N (atoms/cm^3-atmos) in Eq. (4) can be obtained from the perfect gas law, $P_T V = n R'T$, where n is the number of moles and V is the volume (cm^3). Rewriting this with $R' = N_o k$, one obtains $N = n N_o / P_T V = 1/kT$. Hence Eq. (4) becomes

$$S' = 6.45 \times 10^5 f,$$
(A-3)

where f is taken from the tabulated values of Unsöld[1]. The relations for S for the Balmer and Paschen lines, respectively, become from Eq. (6),

$$S = 3.092 \times 10^{-6} [1 - \exp(-1.427 \times 10^{-4} \omega_o)] S',$$

and
(A-4)

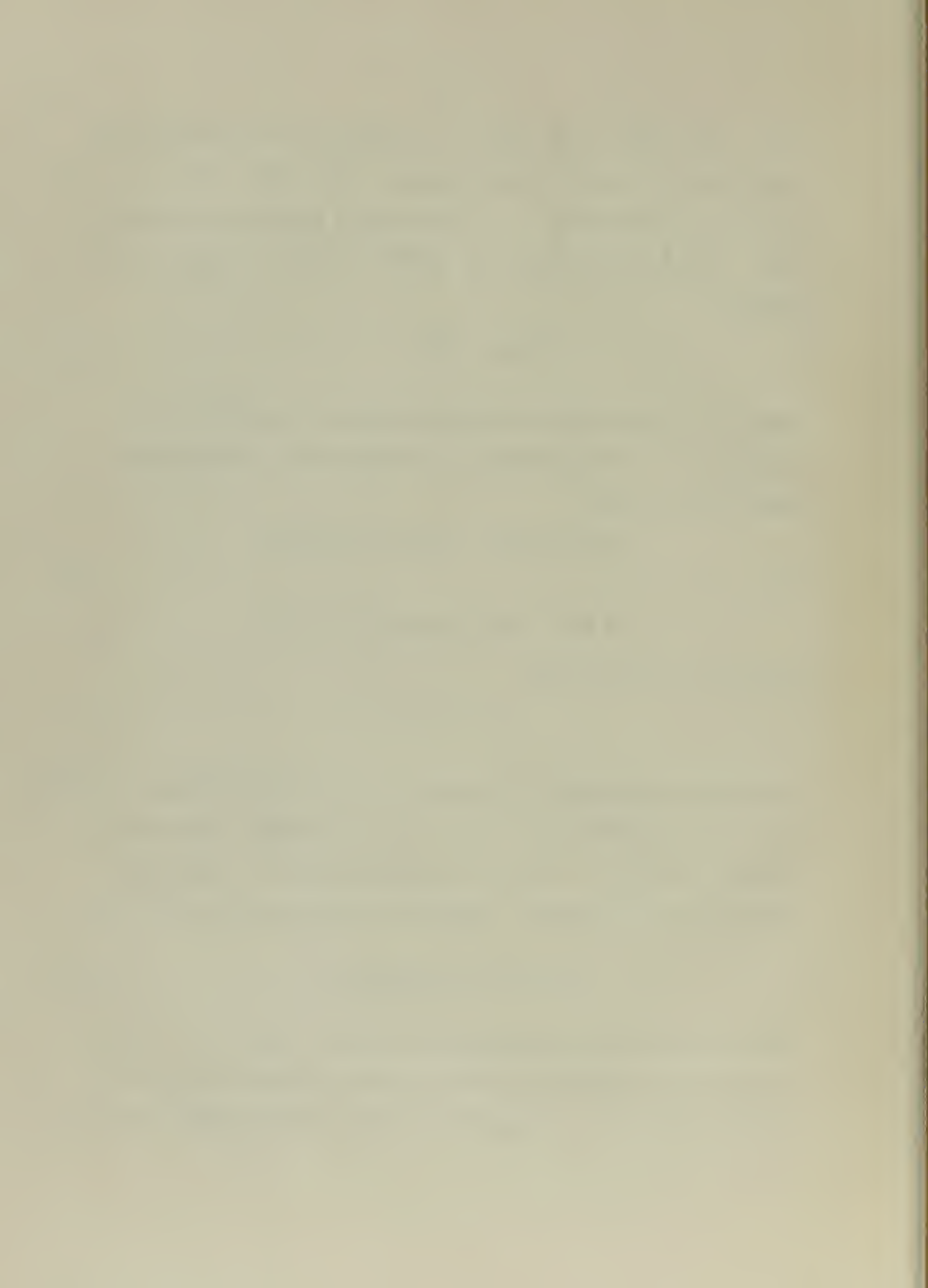$$S = 8.046 \times 10^{-6} [1 - \exp(-1.427 \times 10^{-4} \omega_o)] S'.$$

Equation (2) is then written

$$P' = 1.315 \times 10^4 S/\omega_o.$$
(A-5)

At the given temperature and pressure $b_o = 3.58 \times 10^{-5} \omega_o$ [Eq. (8)], and $a = 4.71 \times 10^4 S'/\omega_o^2$ [Eqs. (7), (8), and (9)]. The terms a and $\log_{10} 10.6 P'X$ can now be determined and S is then found from the curves of growth. The intensity width from Eq. (13) is now

$$2|\omega_\lambda - \omega_o| = 2.403 \, S \, b_o.$$
(A-6)

Table A-III gives the necessary data to obtain $2|\omega_\lambda - \omega_o|$ for the spectral lines considered, and the last column of this table gives the value of $2|\omega_\lambda - \omega_o|$ computed from these data. The additional area

contributed by each line is usually obtained by multiplying $2|\omega_{\hbar} - \omega_o|$ by $(R_{\omega}^o - R_{\omega}^c)$ at ω_o. If $2|\omega_{\hbar} - \omega_o|$ is so large that either R_{ω}^o or R_{ω}^c deviate appreciably from linear variation along the entire intensity width, then the area must be found by graphical methods. These additional areas are listed below:

	Balmer			Paschen	
Line	Area (erg/cm^2-sec)		Line	Area (erg/cm^2-sec)	
3	3.13×10^{10}		4	0.635×10^{10}	
4	0.650		5	0.204	
5	0.224		6	0.125	
6	0.098		7	0.052	
7	0.056		8	0.037	
8	0.037				

The Lyman contribution is taken as blackbody from the left cut-off point ($\omega = 7.46 \times 10^4$) to $\omega = \infty$. This area is found to be 0.250×10^{10} erg/cm^2-sec.

Hence, the total area contributing to the emissivity, i.e., the sum of the continuous spectrum and discrete transition contributions, is 16.43×10^{10} erg/cm^2-sec, and therefore $\epsilon = 1.643 \times 10^{11}/5.85 \times 10^{11} = 0.281$.
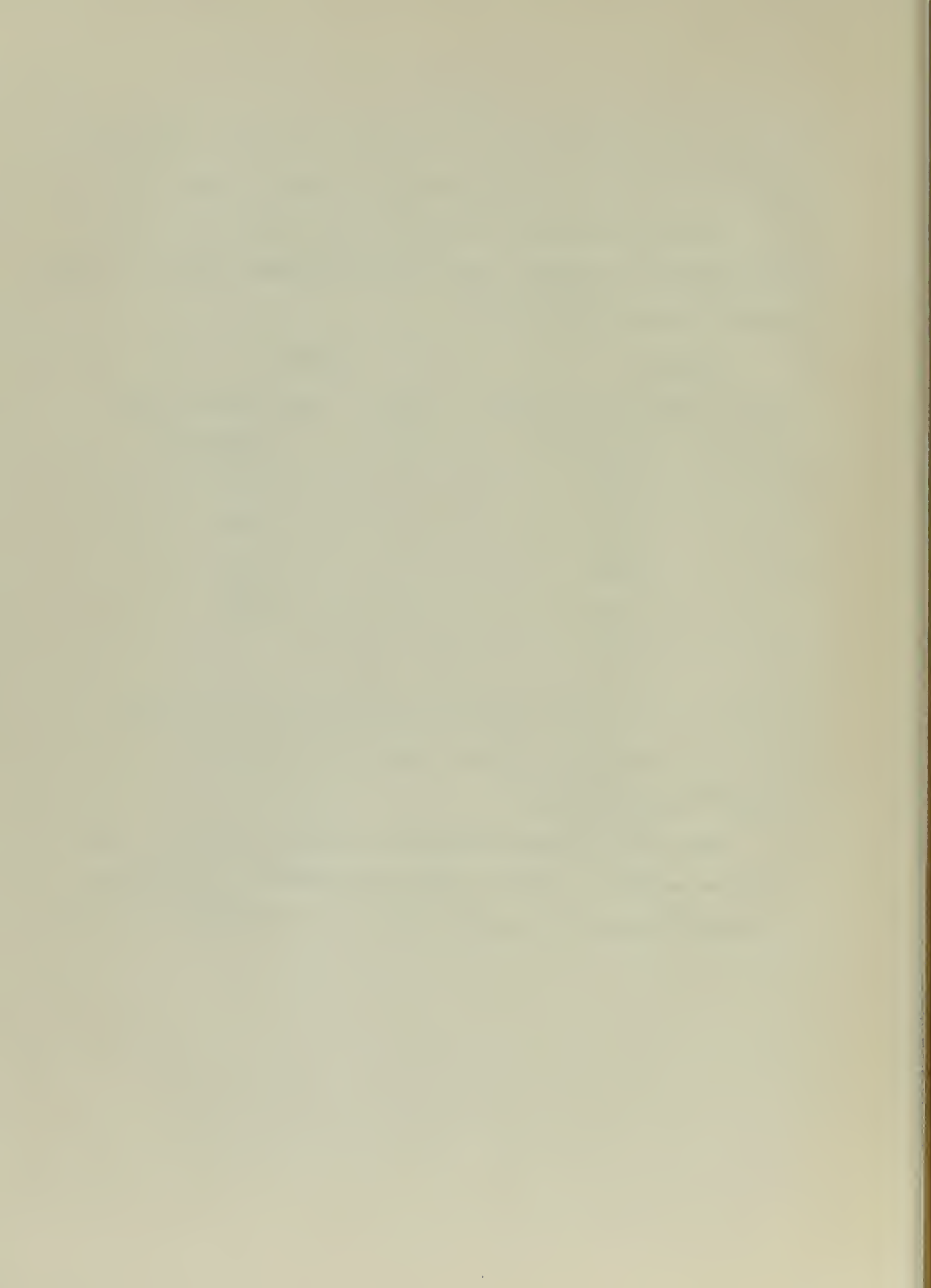
TABLE A-I. $R_\omega^\bullet$ AS A FUNCTION OF ω ($T = 10080^\circ$K).

$\omega/10^3$	$R_\omega^\bullet/10^6$
1	0.244
3	1.90
4.38	3.63
6.85	7.30
10	11.80
12.19	14.40
15	16.83
20	18.22
25	16.94
27.4	15.70
30	14.02
32.5	12.44
35	11.05
40	7.87
45	5.50
50	3.74
60	1.55
70	0.589
80	0.212
90	0.072
100	0.025

TABLE A-II. P_ω^c AND R_ω^c AS FUNCTION OF ω ($T = 10080^\circ K$, $P_T = 40$ ATMOS, $\ell = 50$ CM).

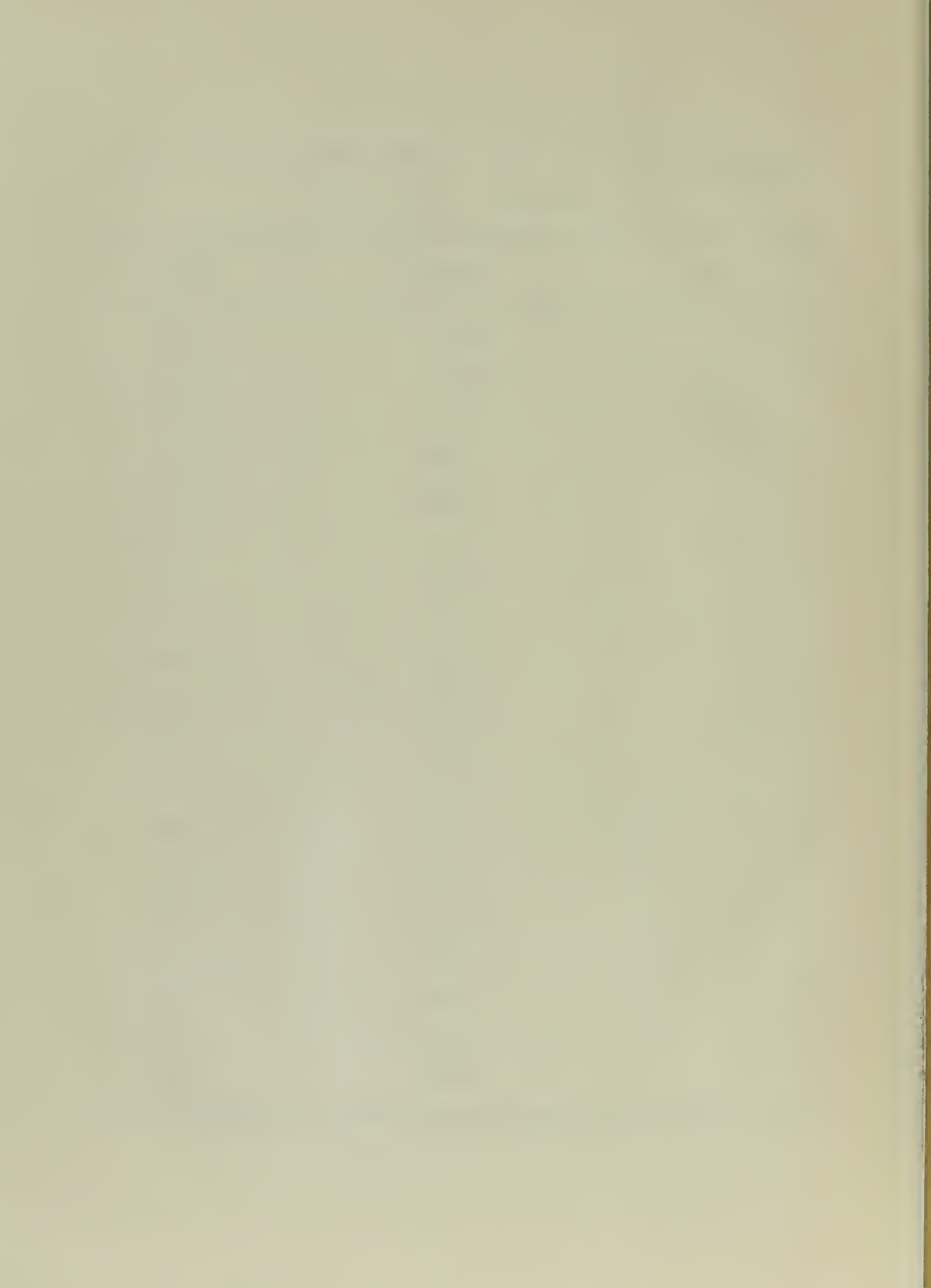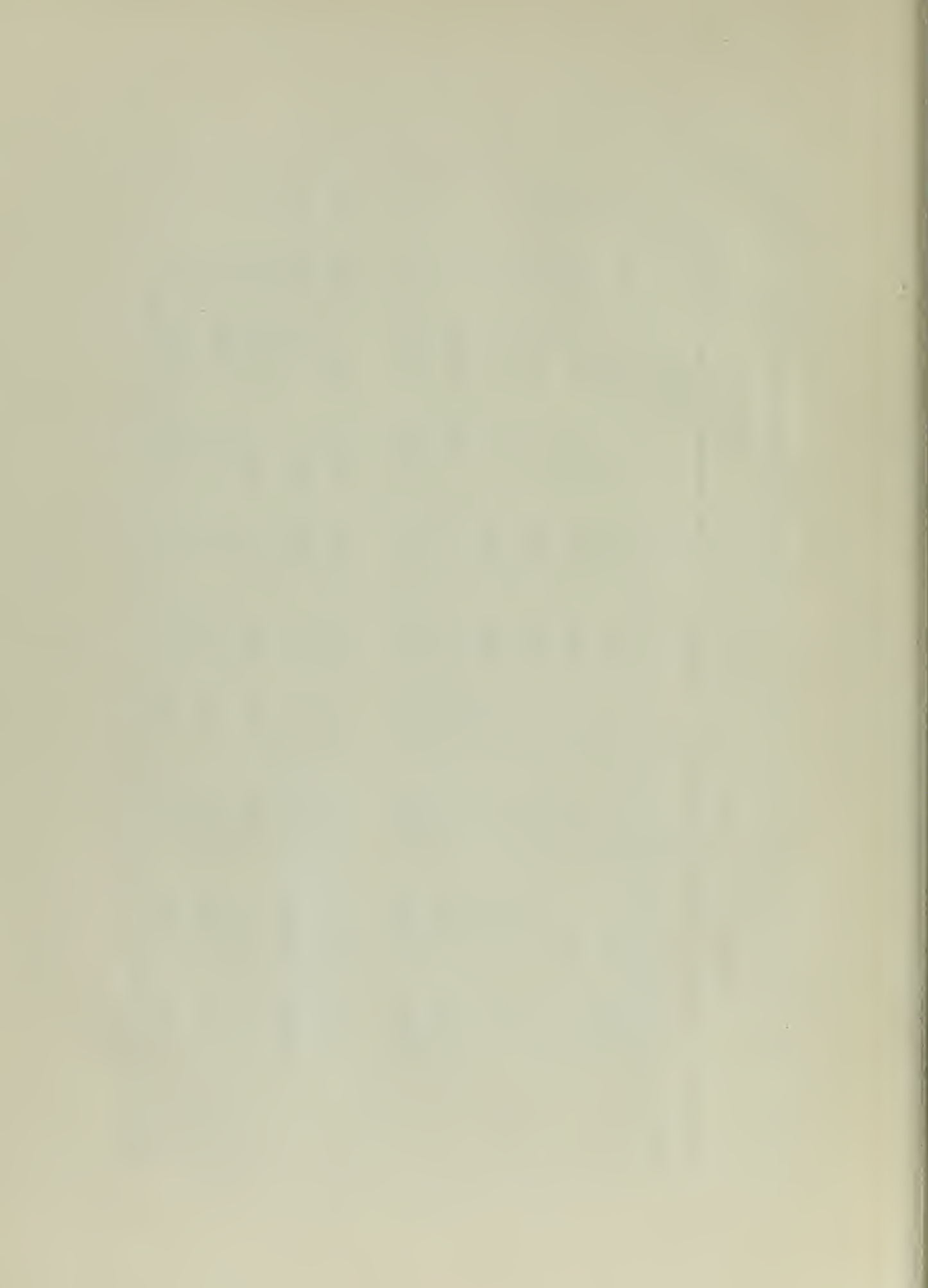| $\omega/10^3$	$P_\omega^c/10^{-4}$	$R_\omega^c/10^6$
4.38	3.82	1.94
6.85	1.35	1.73
6.85	2.29	2.68
10	0.900	1.94
12.19	0.540	1.47
12.19	1.65	4.05
15	0.944	2.90
20	0.426	1.49
25	0.225	0.748
27.4	0.172	0.531
27.4	3.58	8.05
30	2.75	5.94
32.5	2.18	4.40
35	1.75	3.25
40	1.17	1.65
45	0.826	0.839
50	0.600	0.423
60	0.348	0.104
70	0.220	0.025

TABLE A-III. INTENSITY WIDTH AND MISCELLANEOUS DATA FOR COMPUTING INTENSITY WIDTH FOR BALMER AND PASCHEN LINES (T = 10,080°K, P_T = 40, ℓ = 50).

Balmer	$\omega_0/10^4$	f	$S'/10^5$	S	$\cdot P'$	γ_0	α	$10.6^P X/10^4$	γ	$2|\omega_L - \omega_0|$
3	1.522	0.637	4.11	11.24	9.70	0.545	83.5	20.6	1700	2230
4	2.058	0.119	0.767	2.24	1.432	0.736	8.56	3.04	215	380
5	2.305	0.0443	0.286	0.848	0.483	0.825	2.54	1.02	67	133
6	2.440	0.0212	0.137	0.407	0.223	0.859	1.12	0.473	29	60
7	2.515	0.0122	0.079	0.235	0.123	0.900	0.586	0.261	15.5	35
8	2.575	0.0080	0.052	0.155	0.0792	0.920	0.367	0.164	9.6	21
Paschen										
4	0.533	0.841	5.43	2.33	5.74	0.191	898	12.2	4400	2020
5	0.779	0.150	0.967	0.522	0.881	0.279	75.2	1.87	500	336
6	0.913	0.0554	0.357	0.209	0.301	0.327	20.2	0.637	150	118
7	0.994	0.0269	0.174	0.106	0.1403	0.356	8.24	0.297	64	55
8	1.048	0.0161	0.104	0.065	0.0815	0.375	4.46	0.181	39	35